

RESEARCH

Open Access



The microbiota of cork and yellow stain as a model for a new route for the synthesis of chlorophenols and chloroanisoles from the microbial degradation of suberin and/or lignin

Marina Ruiz-Muñoz¹, Ignacio Ontañón², Rebeca Cobos¹, Carla Calvo-Peña¹, Rebeca Otero-Suárez¹, Vicente Ferreira^{2*}, Jordi Roselló³ and Juan José R. Coque^{1*}

Abstract

Background The main application of cork is the production of stoppers for wine bottles. Cork sometimes contains 2,4,6-trichloroanisole, a compound that, at a concentration of ng/L, produces an unpleasant musty odor that destroys the organoleptic properties of wine and results in enormous economic losses for wineries and cork industries. Cork can exhibit a defect known as yellow stain, which is associated with high levels of 2,4,6-trichloroanisole. We describe how the microbiota of cork and yellow stain define a novel mechanism that explains the formation of chlorophenols and chloroanisoles (including 2,4,6-trichloroanisole) from *p*-hydroxybenzoate produced during lignin and/or suberin breakdown.

Results Electron microscopy revealed that cork affected by yellow stain exhibited significant structural degradation. This deterioration was attributed to the presence of higher microbial populations compared to those found in standard cork. Cork microbiota is rich in filamentous fungi able to metabolize lignin. A metataxonomic analysis confirmed that yellow stain contained significantly greater populations of fungal species belonging to *Absidia*, *Geomyces*, *Mortierella*, *Mucor*, *Penicillium*, *Pseudogymnoascus*, *Talaromyces*, and *Umbelopsis*. It also contained significantly greater amounts of bacteria belonging to Enterobacterales, Streptosporangiales, Tepidisphaerales, *Pseudomonas*, and several members of Burkholderiaceae, particularly species of the *Burkholderia-Caballeronia-Paraburkholderia* group. The extraction of aromatic compounds from cork samples allowed the identification of several compounds typically observed following lignin depolymerization. Notably, *p*-hydroxybenzoic acid and phenol were detected. Two strains of the genus *Streptomyces* isolated from yellow stain were able to biotransform *p*-hydroxybenzoate into phenol in resting cell assays. Phenol could be efficiently chlorinated in vitro to produce 2,4,6-trichlorophenol by a fungal chloroperoxidase, an enzymatic activity commonly found in filamentous fungi isolated from cork. Finally, as has been

*Correspondence:

Vicente Ferreira

vferre@unizar.es

Juan José R. Coque

jjrubc@unileon.es

Full list of author information is available at the end of the article



© The Author(s) 2025. **Open Access** This article is licensed under a Creative Commons Attribution-NonCommercial-NoDerivatives 4.0 International License, which permits any non-commercial use, sharing, distribution and reproduction in any medium or format, as long as you give appropriate credit to the original author(s) and the source, provide a link to the Creative Commons licence, and indicate if you modified the licensed material. You do not have permission under this licence to share adapted material derived from this article or parts of it. The images or other third party material in this article are included in the article's Creative Commons licence, unless indicated otherwise in a credit line to the material. If material is not included in the article's Creative Commons licence and your intended use is not permitted by statutory regulation or exceeds the permitted use, you will need to obtain permission directly from the copyright holder. To view a copy of this licence, visit <http://creativecommons.org/licenses/by-nc-nd/4.0/>.

widely demonstrated before, 2,4,6-trichlorophenol can be efficiently *O*-methylated to 2,4,6-trichloroanisole by many of fungi that inhabit cork.

Conclusions Chlorophenols and chloroanisoles can be produced *de novo* in cork from *p*-hydroxybenzoate generated by the microbial biodegradation of lignin and/or suberin through the participation of different types of microorganisms present in cork. The natural origin of these compounds, which are of great interest for the chlorine cycle and represent a new source of environmental contamination that differs from that caused by human activity, is described.

Keywords Cork, Microbiome, Yellow stain, Lignin, Suberin, Chlorophenols, Chloroanisoles, 2,4,6-Trichloroanisole, Fungi, Bacteria

Background

Cork, a renewable and biodegradable biopolymer of vegetable origin, is derived from the bark of the cork oak (*Quercus suber* L.), which is typically harvested every 9–12 years [1]. The primary application of cork is the production of stoppers for wine bottles, particularly for high-quality wines. This preference is due to cork's notable properties, including its stability, non-toxicity, low permeability to liquids and gases, and remarkable mechanical elasticity [2, 3]. According to Pereira [4], the chemical composition of cork consists mainly of suberin (42.8%) and lignin (22.0%). Additionally, minor components include polysaccharides and other extractable chemical compounds (16.0%). These extractable compounds encompass a diverse array of nonpolar substances, such as long-chain lipids and triterpenes, as well as polar compounds, primarily low- and high-molecular-weight phenolic compounds, which constitute the majority of the potentially soluble compounds in cork. Lignin is a complex 3-dimensional heterogeneous biopolymer formed by the radical polymerization of three monolignols, including *p*-coumaryl, coniferyl, and sinapyl alcohols [5]. The microbial depolymerization of lignin generates a diverse array of phenolic compounds, including syringyl, guaiaicyl, and *p*-hydroxyphenyl units. These compounds can undergo microbial degradation to yield syringate, vanillate, and *p*-hydroxybenzoate, respectively [6]. Additionally, this process also produces other compounds such as benzoic acid, benzaldehyde, cinnamic acid, acetophenone, and various phenol derivatives (among others) [7, 8]. Suberin is a cell wall polymer described as a polyester of predominantly aliphatic monomers (different types of fatty acids esterified with glycerol), phenolic-derived compounds (mainly hydroxycinnamic ferulic acid and tyramine), and glycerol [9, 10]. Suberin depolymerization, through various ester cleavage techniques, results in a mixture of insoluble polyaromatic compounds, cosoluble phenolic compounds, and aliphatic suberin monomers [11]. Among the soluble phenolics detected, hydroxycinnamic ferulic acid consistently appears in relatively high quantities, whereas tyramine is present in relatively low

amounts [12]. Consequently, the microbial degradation of lignin and suberin generates a diverse array of simple aromatic compounds.

Occasionally, cork can develop a defect, or yellowish stain, known as yellow stain (YS) or yellow spot (Fig. 1). YS predominantly develops on the back of the cork bark, particularly in areas where the bark contacts the ground, and may also cause discoloration of the adjacent cork tissue [13]. Scanning electron microscopy (SEM) studies of healthy, or standard cork (SC), and cork affected by YS have revealed distinct differences in cellular structures. The tissues impacted by YS exhibited deformed, wrinkled



Fig. 1 Yellow stain (YS) spots (indicated by arrows) located under the bark of a cork plank

cells with cell wall separation at the middle lamella level [14]. These changes were related to the degradation of lignin and pectin, as evidenced by the deposition of calcium in the intercellular space of the attacked cells [14]. Comparative chemical studies have demonstrated that cork affected by YS undergoes degradation of the phenolic matrix, resulting in discoloration [15] and higher levels of 2,4,6-trichloroanisole (2,4,6-TCA) [1, 16]. This is particularly significant because 2,4,6-TCA contamination in cork stoppers can migrate into wine, producing an unpleasant off-odor characterized by moldy, musty, and earthy aromas. These odors can mask the natural wine aromas and compromise its organoleptic properties, a defect commonly referred to as “cork taint” [17–19]. The issue of 2,4,6-TCA taint poses a substantial problem for the cork and wine industries, resulting in annual losses exceeding 10 billion dollars [20]. It is now widely accepted that the majority of 2,4,6-TCA contamination in cork arises from an *O*-methylation reaction of the pesticide (fungicide) 2,4,6-trichlorophenol (2,4,6-TCP), carried out by various microbial species, predominantly filamentous fungi inhabiting cork [17, 21, 22]. This reaction is catalyzed by an inducible chlorophenol-*O*-methyltransferase (CPOMT), which has been characterized from a *Trichoderma longibrachiatum* strain isolated from cork, although proteins with high homology have been found in many other fungal species [23, 24]. From a physiological perspective, this reaction is crucial for microorganisms as it converts the highly toxic pesticide 2,4,6-TCP into the nontoxic compound 2,4,6-TCA, thereby enabling their survival [17]. Chlorophenols (CPs), notably 2,4,6-TCP and pentachlorophenol (PCP), have been extensively employed for decades as fungicides, primarily as wood preservatives, as well as herbicides and defoliant on a global scale. Consequently, CPs are now prevalent contaminants in various ecosystems, including surface and groundwater, bottom sediments, atmospheric air, and soil [25, 26]. As a result, they have been recognized as significant pollutants in countries such as the United States and China [27, 28]. Chloroanisoles (CAs) are produced through *O*-methylation reactions from their precursors, the chlorophenolic pesticides. Consequently, CAs have become prevalent contaminants across various ecosystems, including bottom sediments [29]; surface and groundwater [30, 31]; atmospheric air and soils [32, 33]; vegetable materials, such as the bark of the cork-oak in Mediterranean forests [34]; and even as indoor pollutants in Swedish houses [35]. Thus, it is currently assumed that cork bark can gradually adsorb 2,4,6-TCP from the environment (via the atmosphere, soil, or rain). This compound is subsequently detoxified by the numerous filamentous fungi inhabiting the bark, converting it into

the nontoxic 2,4,6-TCA, which remains strongly bound to the lipid matrix of suberin due to its lipophilic nature.

However, certain indications might suggest the existence of alternative mechanisms for the production of 2,4,6-TCA on cork, beyond the previously mentioned mechanism. These indications include the presence of relatively high levels of 2,4,6-TCA in cork affected by YS. Notably, wines with a pronounced “cork taint” character were first described in 1904 [36], many years before the industrial production of the first chlorophenolic pesticides. The industrial production of the first CPs began in 1936 with the commercial use of PCP as an antiseptic [37].

Also, we should mention that once removed from the tree, cork slabs are, in most cases, immediately transported to the cork factories where they are stored until further processing. Next, the cork slabs are boiled for approximately 1 h to soften them and facilitate the mechanical extraction of the corks. After boiling, the slabs are left to stand in piles for 1–3 weeks to flatten. Once the water content is optimal, the slabs are processed into cork stoppers. During this period of 1–3 weeks, fungi rapidly proliferate on the slabs, leading to an increase in 2,4,6-TCA levels, even in the absence of exogenous 2,4,6-TCP contamination [15], as is well known in all cork factories. These observations have led some researchers to hypothesize that 2,4,6-TCA could be formed from phenol, which could be endogenously synthesized from glucose via the pentose phosphate and shikimic acid pathways. Subsequently, phenol may undergo extracellular chlorination mediated by chlorine-containing agents, resulting in the production of various CPs, including 2,4,6-TCP [38]. However, this mechanism is highly unlikely because, to the best of our knowledge, microbial phenol formation from shikimic acid has not been documented. Additionally, the use of hypochlorite as a cork bleaching agent was banned around 1990 and has since been completely abandoned by all cork stopper producers [19].

Finally, many different studies have extensively characterized the microbial populations present on cork throughout various stages of the production process [17, 21, 22, 39–41], to mention the most recent. However, investigations into the microbial populations associated with the YS have been limited. This gap was addressed by Veloso and colleagues [42], who identified a significant correlation between the genus *Trichoderma*, specifically a strain of *Trichoderma atrobrunneum*, and elevated levels of 2,4,6-TCA in the YS.

This study focuses on the characterization of bacterial and fungal populations associated with standard cork (SC) and cork affected by the YS using a metataxonomic approach. A metabolomic approach was employed to

detect aromatic compounds associated with cork, while classical microbiological techniques were utilized to isolate various fungal and bacterial strains to analyze their potential involvement in lignin degradation and aromatic compounds metabolism. Our research has identified a novel “natural” process that elucidates the biosynthesis of CPs and CAs from aromatic substrates generated during the microbial biodegradation of lignin and/or suberin in cork affected by the YS.

Methods

Cork sampling and isolation of microorganisms

Cork samples (planks of approximately 20×20 cm) were taken from five different trees in a forest located near the village of Cassá de la Selva (Gerona, Spain) (41°53′50.7″N 2°53′24.0″E). The samples were taken from the area where the trunk touches the ground and where the presence of the YS is most common. The samples were visually inspected to confirm the presence or absence of YS. The cork samples were placed in sterile plastic bags and transported cold (4 °C) to the laboratory, where they were stored at the same temperature until processing.

Filamentous fungi were isolated from 1-g samples of standard cork (SC) or YS. The cork was cut into small fragments via a sterile scalpel and placed in a 50-mL Falcon tube containing 10 mL of sterile saline solution (NaCl 0.9%). The samples were vortexed for 2 min and then incubated at room temperature (RT) in a rotary incubator for up to 2 h. To isolate filamentous fungi, tenfold dilutions were spread on the surface of rose bengal chloramphenicol (RB) agar (Condalab, Torrejón de Ardoz, Spain), potato dextrose (PDA) agar (Merck KGaA, Darmstadt, Germany), and malt extract (MEA) agar (Condalab). The last two media were supplemented with chloramphenicol (150 µg/mL) to inhibit bacterial growth.

Plates were incubated at 25 °C in the dark for up to 10 days. For the isolation of aerobic mesophilic bacteria, tenfold serial dilutions were plated on agar plates of plate count agar (PCA) (Merck KGaA) and incubated at 30 °C for up to 7 days. Actinobacteria were isolated on starch casein agar (SCA) plates [43] incubated at 28 °C for up to 14 days. Sporulated bacilli were isolated from cork samples heated at 80 °C for 30 min and then spread on PCA plates and incubated at 30 °C for 5 days. Enterobacteriaceae were isolated by plating on McConkey agar (Condalab) plates and incubated at 30 °C for up to 5 days. All media used for bacterial isolation were supplemented with pimarinin (100 µg/mL) to prevent fungal growth. Microorganisms with the ability to metabolize vanillic acid were selected on plates of agar minimal medium

containing vanillic acid and bromothymol blue as previously described [39].

Scanning electron microscopy (SEM) and transmission electron microscopy (TEM)

Cork samples for SEM were cut with a razor blade, and small blocks were fixed with 2% glutaraldehyde in 0.1-M phosphate buffer (pH 7.4) for 12 h at 4 °C. The samples were washed in buffer and postfixed in 1% osmium tetroxide solution in 0.1-M phosphate buffer (pH 7.4) for 2 h in the dark. The samples were dehydrated in graded ethanol solutions (30%, 50%, 70%, 90%, 3×96%, and 3×100%, each for 8 h). They were dried in a critical-point drying apparatus (CPD300, Leica, Wien, Austria) with liquid CO₂, mounted on aluminum stubs with conductive carbon tape, and sputter-coated with gold palladium (ACE200, Leica, Wien, Austria). The samples were observed under a JEOL JSM-6840LV scanning electron microscope (JEOL, Tokyo, Japan) at 20 kV.

For TEM analysis, samples (cork blocks of 1 mm³) were fixed with 2% glutaraldehyde in 0.1-M phosphate buffer (pH 7.4) for 24 h at 4 °C and rinsed with this buffer. The samples were then postfixed with a buffered osmium tetroxide solution (1%) for 3 h at room temperature and washed in buffer again. The samples were dehydrated through a graded series of ethanol solutions (30%, 50%, 70%, 90%, 3×96%, and 3×100%, each for 8 h). The samples were then embedded in Epon 812 resin (Polysciences, Eppelheim, Germany) for several days, after which the resin was polymerized at 60 °C for 24 h. The samples were trimmed, and ultrathin sections were obtained and stained with toluidine blue (0.5% in an aqueous solution). The ultrathin sections were mounted on 200-mesh grids and contrasted with UranylLess and lead citrate (EMS, Hatfield, USA). Finally, the ultrathin sections were observed with a JEOL 1010 electron microscope (JEOL, Tokyo, Japan) operating at 80 kV.

Molecular identification of microorganisms isolated from cork

Total genomic DNA from the isolates was extracted via PrepMan™ Ultra Sample Preparation Reagent (Applied Biosystems, Carlsbad, CA, USA) according to the manufacturer's instructions. Fungal isolates were identified to the genus level by sequencing their internal transcribed spacer 1 (ITS1)–5.8 S-ITS2 regions via the ITS1 and ITS4 primers [44]. On the other hand, bacterial isolates were identified via partial sequencing of a region of the 16S rRNA gene via primers 27F and 1492R [45], and contigs were generated from both sequences via BioEdit (v.7.2) [46]. Isolates were identified via sequence comparison via BLASTn (NCBI GenBank database) (<http://www.ncbi.nlm.nih.gov/BLAST>).

Identification was considered if the sequence had an identity $\geq 98\%$ and a query coverage $\geq 90\%$.

DNA extraction from cork samples and sequencing for metataxonomic analysis

Approximately, 1 g of cork was collected from each sample as described above and cut into small fragments of 1–2 mm in average size via a sterile scalpel. These samples were then crushed in a mortar in the presence of liquid nitrogen to obtain a powder. Total genomic DNA was then isolated from 500 mg of cork powder via the NZYSoil gDNA Isolation Kit (NZYTech, Lisbon, Portugal) according to the manufacturer's instructions. The concentration of the purified DNA was measured via a Qubit fluorometer (Thermo Fisher Scientific, Waltham, MA, USA) before being sent to FISABIO (Valencia, Spain) for sequencing.

DNA samples from both fungal and bacterial populations were amplified via primers designed around conserved regions. For fungi, PCR amplification targeted the ITS2 region within the fungal nuclear ribosomal DNA (rDNA) via the primers ITS3_KYO2 and ITS4 [47], whereas for bacteria, the V4 region of the 16S rRNA gene was targeted via the primers 515F and 806R [48]. DNA amplicon libraries were generated via the following PCR cycle: initial denaturation at 95 °C for 3 min, followed by 28 cycles of annealing (95 °C for 30 s, 55 °C for 30 s, and 72 °C for 30 s) and a final extension at 72 °C for 5 min, with KAPA HiFi HotStart ReadyMix (Roche, Indianapolis, IN, USA). Illumina sequencing adapters and dual index barcodes (Nextera XT index kit v2, FC-131–2001) were then added to the amplicons. Libraries were normalized and pooled prior to sequencing. The pool of indexed amplicons was loaded onto the MiSeq Reagent Cartridge v3 (MS-102–3003) spiked with 25% PhiX control to enhance base calling during sequencing, as recommended by Illumina for amplicon sequencing.

Data analysis of the high-throughput amplification assay

Forward and reverse reads obtained from the Illumina sequencing platform were subjected to quality analysis via the fastp program [49] with a minimum read length of 50, a minimum trim quality average of 20, and a window size of 10 bp. DNA amplicons from both fungal and bacterial populations were then processed to infer the amplicon sequence variants (ASVs) present in each cork sample via the DADA2 package [50]. ASVs, as opposed to operational taxonomic units (OTUs), which are defined at fixed thresholds, provide a more accurate, consistent, and reproducible representation of the amplicon sequence community [51]. For raw ITS rRNA reads, the first step involved trimming the adapter sequences and removing primer residues via cutadapt [52]. The reads

were then filtered via DADA2 on the basis of the recommended criteria, which included removing uncalled bases, allowing a maximum of 2 expected errors, and truncating reads with a quality score of 2 or less. Taxonomic classification of the ITS rRNA sequences was then performed via the UNITE database v18.11.2018 [53]. Similarly, for the raw 16S rRNA reads, filtering procedures were applied prior to taxonomic assignment against the SILVA database v.138.1 [54] via DADA2-formatted training files for taxonomy. Furthermore, ASVs with a frequency of fewer than 10 reads in all samples were excluded from both datasets to minimize potential noise and increase the reliability of subsequent analyses.

Microbial diversity, taxonomy distribution, and statistical analysis

The α -diversity of the inferred ASVs was assessed via the Chao1, Shannon, and Gini–Simpson indices, which were calculated via the phyloseq package (v.1.48.0) [55]. Pielou's evenness index [56] was also calculated. Wilcoxon rank-sum tests were performed to assess significant differences between diversity indices, with a significance level of 0.05. β -diversity was examined via a PERMANOVA nonparametric test [57] with 9999 permutations to determine whether community composition varied between experimental conditions. Principal coordinate analysis (PCoA) based on Bray–Curtis dissimilarity was used to assess the structural relationships of microbial communities between samples. These analyses were performed via the phyloseq v.1.48.0 and Vegan v.2.6–6.1 packages [55, 58]. To account for potential bias and to normalize sample data, negative binomial distribution normalization was implemented in the DESeq2 package (v.1.44.0) [59]. Pairwise differential abundance analysis was then performed on count data, using a significance level of 0.01. p -values were adjusted via the false discovery rate (FDR) method [60]. In addition, Wilcoxon signed-rank tests were performed to assess significant differences between the relative abundances of the taxa found, with a significance level of 0.05. All the statistical analyses were performed in R (v. 4.3.3) [61] via RStudio (v. 2023.03.0).

Extraction and analysis of phenolic compounds from cork

Ten grams of each of the five cork samples were crushed and ground at room temperature to a particle size $< 200 \mu\text{m}$ via a ZM 200 ultracentrifugation mill (Retsch, Haan, Germany). For the extraction procedure, 2.4 g of cork powder from each sample was weighed and placed in a Pyrex bottle, to which 100 mL of 12% hydroalcoholic solution (adjusted to pH 12 with NaOH) was added. The mixture was macerated for 24 h at room temperature in a linear shaker with gentle stirring (300 rpm).

The sample was then centrifuged at 4500 rpm at 8 °C for 10 min, the supernatant was filtered with filter paper (Scharlab, Sentmenat, Spain), and the pH was adjusted to 5.6 with a 0.37% HCl solution. The extract was percolated through 100 mg of Bond Elut ENV cartridges (Agilent Technologies, Santa Clara, CA, USA), which were previously conditioned by passing 4 mL of dichloromethane, followed by the addition of 4 mL of methanol and 4 mL of Milli-Q water. The cartridges were then dried under vacuum and eluted with 4 mL of ethanol. The extracts were dried under a nitrogen stream and redissolved in 300 µL of ethanol.

Seven microliters of each extract was injected into a UHPLC (ESI)-TIMS-QTOF-MS from Bruker Daltonics (Billerica, MA, USA) using an ACQUITY UPLC BEH C18 column (100×2.1, 1.7 µm) from Waters (Milford, MA, USA), which was held at 35 °C during the analysis, whereas the samples were kept at 8 °C throughout the analysis. The flow rate was 0.3 mL/min, and the mobile phases used were Milli-Q water (A) and acetonitrile (B) with 0.1% formic acid. The gradient used was as follows: 0–3.5 min, 95% mobile phase A isocratic; 3.5–8.7 min, 95–55% A; 8.7–11.3 min, 55–35% A; 11.3–13.4 min, 35–10% A; and 13.4–18.4 min, 10% A isocratic.

The samples were analyzed in negative ESI mode over a mass range of 20–1300 amu. The source parameters were as follows: capillary, 3 kV; end plate offset, 500 V; nebulizer, 4 bar; dry gas (nitrogen), 8 L/min; and drying temperature, 200 °C. All samples were analyzed in MS mode with a scan duration of 0.3 s in centroid mode, and tandem mass spectrometry (MS/MS) was carried out with a mixture of all samples (10 µL of each extract was mixed before the analysis) in Auto MS/MS mode and with a scheduled precursor list for some selected molecular ions using collision energies ranging from 20 to 50 eV. Chromatograms were processed via Bruker MetaboScape 2023b software. Parameters used for alignment and peak picking were performed in default mode by MetaboScape. It has only extracted the features which appeared in, at least, the half of the samples. The intensity threshold was 1000 counts, and the mass range from 90 to 600 *m/z*. The first minute and the last 5 min of the run were excluded from data processing.

Screening of filamentous fungi for detection of lignin-degrading capabilities

To test lignin-utilizing and/or lignin-degrading capabilities, the isolated fungal strains were cultured on plates containing Highley's minimal medium (HMM) supplemented with 5 g/L Kraft lignin (Sigma–Aldrich, Saint Louis, MO, USA) as the sole carbon source [62]. The isolates were cultured at 25 °C in the dark for up to 14 days, and growth was recorded on days 7 and 14

post-inoculation. The screening process also included the use of decolorizing dyes, which change color due to the production of lignin-degrading enzymes. The decolorizing dyes used were 2,2-azino-bis (3-ethylbenzothiazine-6-sulfonic acid) (ABTS), reactive black 5 (RB5), and Remazol Brilliant Blue R (RBBR). ABTS is a nonphenolic dye that is oxidized by laccases to form a more stable cationic radical, resulting in a blue–green color that correlates with enzyme activity [63]. Decoloration of both RBBR and RB5 is a result of the production of peroxidases such as lignin peroxidase (LiP), manganese peroxidase (MnP), or versatile peroxidase (VP) [64, 65]. To test the ligninolytic enzyme production of the fungal isolates, they were cultured on HMM agar plates supplemented with 0.2% glucose as the carbon source and decolorizing dyes consisting of 2-mM ABTS, 50 mg/L RB5, or 200 mg/L RBBR. The dyes were filtered through a 0.2-µm filter for sterilization and added to the agar medium. The plates were incubated at 25 °C in the dark for up to 14 days, and decolorization was recorded at 3, 7, and 14 days after inoculation.

Detection of chloroperoxidase (CPO) activity in fungal liquid cultures

Fungal strains were grown for 72–96 h at 25 °C on an orbital shaker (200 rpm) in 500-mL Erlenmeyer flasks containing 100 mL of CFM liquid medium [66]. The flasks were inoculated with 10 agar plugs (9 mm in diameter) from a fungal culture previously grown on PDA plates. CPO activity was tested by using a phenol red-based colorimetric assay [66]. Briefly, 700 µL of each culture was mixed with an equal volume of a reaction mixture containing 0.008% (w/v) phenol red added from a 0.2% stock mixture in 95% ethanol, 0.3-M potassium phosphate buffer (pH 7.0), and 0.05-M sodium chloride. Reactions were initiated by the addition of 10 µL of freshly prepared 0.3% (v/v) hydrogen peroxide and incubated at 25 °C for 1 h. Negative controls were performed in parallel by omitting hydrogen peroxide. All the samples were subsequently centrifuged at 12,000 rpm for 10 min to remove fungal mycelium. CPO activity in the supernatants was determined spectrophotometrically at 595 nm relative to a reaction mixture containing CFM liquid medium.

In silico analysis of CPO taxonomic distribution

To analyze the taxonomic distribution of CPO enzymes in fungal and bacterial taxa, a comprehensive search of the UniProt database (<https://www.uniprot.org/>) was performed in July 2024. The search was performed via the terms “heme haloperoxidase” and “chloroperoxidase” for heme-dependent CPO and “vanadium haloperoxidase” and “vanadium chloroperoxidase” for

vanadium-dependent CPO, with queries restricted to the fungal and bacterial kingdoms. Detailed annotations, including functional descriptions and taxonomic information, were extracted for each protein. This included compiling organism names, taxonomic identifiers, and their classification within fungal and bacterial phyla. The data were then analyzed to determine the distribution of CPOs across different fungal and bacterial groups.

Bioconversion of *p*-hydroxybenzoate to phenol in resting cell systems

The two strains of the genus *Streptomyces* were grown in 500-mL Erlenmeyer flasks containing 100 mL of ISP2 medium [67] for 72 h at 28 °C and 200 rpm in an orbital shaker. The flasks were inoculated with 10 agar plugs (9-mm diameter) of the bacterial strains growing on TBO (tomato paste–oatmeal agar) plates [68]. The cells were recovered via centrifugation under sterile conditions and washed twice at RT with 50 mL of 0.9% NaCl. The cells were then resuspended in 10 mL of 25-mM phosphate buffer (pH 7.0) containing 12-mM *p*-hydroxybenzoate (Thermo Fisher Scientific). The resting cells (1 mL) were incubated with agitation (300 rpm) at 30 °C in a Thermomixer Compact (Eppendorf SE, Hamburg, Germany) for up to 24 h. The reactions were stopped by adding 1 mL of methanol and 10 µL of formic acid to acidify the samples. After centrifugation at 10,000 rpm for 30 min, the culture supernatants were analyzed by high-performance liquid chromatography (HPLC).

The samples for HPLC analyses were filtered through 0.45-µm pore Corning® Costar® Spin-X® centrifuge tube filters (Merck KGaA, Darmstadt, Germany) and stored at –20 °C until analysis. The samples were injected (10 µL) and separated on a LiChospher RP18 analytical column (40×250 mm; 5 µm) (Teknokroma, San Cugat del Vallés, Spain) with acetonitrile–water–formic acid (20:80:1) as the mobile phase at a flow rate of 1 mL/min. Peaks were detected at 275 nm via an Agilent 1200 Series Gradient HPLC System (Agilent Technologies) equipped with a quaternary pump delivery system (G1311A), a preparative autosampler (G1329A), a diode array multiwavelength detector (G7115A), and an analytical fraction collector (G1364F) equipped with an autosampler thermostat (G1330B). Phenol (Across Organics, Monterrey, Mexico) was identified from the retention time and the UV–VIS spectra of the corresponding commercial standard compounds. Quantification was performed by determining the peak areas and interpolating them from standard curves obtained from commercial phenol

dissolved in methanol at concentrations ranging from 10 mg/mL to 10 µg/mL.

In vitro reactions with CPO by using phenolic compounds as substrates

To analyze the ability of CPO to form CAs and CPs, a reaction assay was performed according to Wang and colleagues [69] with slight modifications. The reaction was carried out in 100-mM phosphate buffer (pH 3.0) containing 1-mM NaCl, the substrates (250 µg/mL), and 5-mM H₂O₂ in a total reaction volume of 0.5 mL. Next, 1 µL of commercial CPO solution from *Caldaromyces fumago* with an enzymatic activity of 3000 units/mL (Sigma–Aldrich) was added to start the reaction. Two types of controls (without the addition of CPO or H₂O₂) were also used for each substrate. The reactions were incubated for 1 h at 25 °C in the dark at 600 rpm, and 0.5 mL of methanol was immediately added to the mixtures to stop the reaction. The samples were then filtered and analyzed via HPLC as described above. In this case, the gradient mobile phase consisted of acetonitrile (A) and H₂O containing 0.1% formic acid (B) at a flow rate of 1 mL/min, with an elution gradient consisting of 30% mobile phase A for the first 5 min, then a linear increase to 100% mobile phase A over 40 min, then a return to 30% mobile phase A in 1 min, and finally holding 30% mobile phase A for 5 min for re-equilibration. The substrates employed in such reactions were anisole, phenol, and various other CPs and CAs, namely, 2-chloroanisole (2-CA), 4-chloroanisole (4-CA), 2,4-dichloroanisole (2,4-DCA), 2,6-dichloroanisole (2,6-DCA), 2-chlorophenol (2-CP), 4-chlorophenol (4-CP), 2,4-dichlorophenol (2,4-DCP), and 2,6-dichlorophenol (2,6-DCP). In addition, 2,4,6-TCA, 2,4,6-TCP, 2,3,5,6-tetrachloroanisole (TeCA), 2,3,5,6-tetrachlorophenol (TeCP), pentachloroanisole, and pentachlorophenol (PCP) were also used as standards to measure the compounds formed during the reactions. All chemical compounds were purchased from Sigma–Aldrich, except 2,3,5,6-TeCP (Merck), pentachloroanisole, and PCP (Chem Service Inc., West Chester, PA, USA). The products formed were identified according to their retention time and UV–VIS spectrum by comparison with those of the corresponding standard commercial compounds. Quantification was carried out by determining the peak areas and interpolating them from standard curves obtained from commercial compounds dissolved in methanol at concentrations ranging from 10 mg/mL to 10 µg/mL.

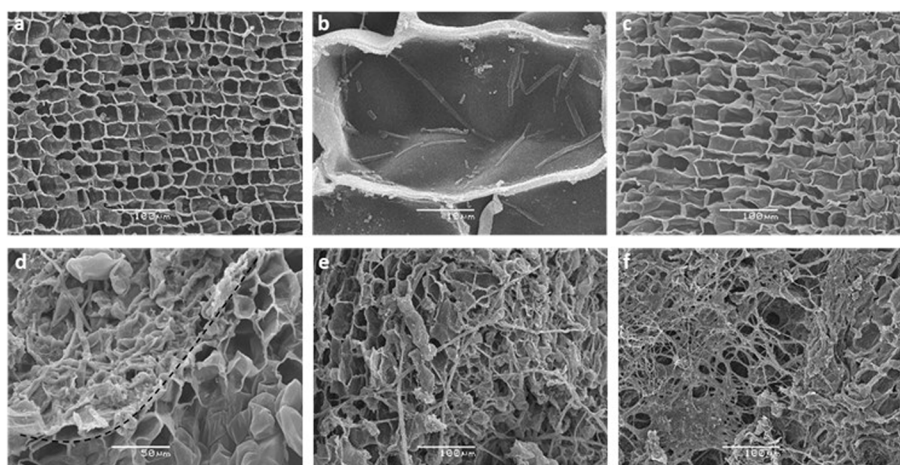


Fig. 2 SEM visualization of the structure of standard cork and yellow stain. SEM photographs of tangential sections of standard cork (**a, b**) display the typical honeycomb arrangement of cork cells, with microorganisms colonizing the interior of cells in **b**. In contrast, cork affected by yellow stain (**c, d, e, f**) shows significant structural degradation. **c** Illustrates the loss of the typical cork structure, with cells wrinkling and collapsing at the right side of photograph. Yellow stain-affected cork exhibits intense microbial colonization, particularly with filamentous fungi (**d, e, f**). The dashed line in photograph **d** could indicate the progression of microbial colonization; to the left, the normal cork structure is completely lost, while to the right, cork cells begin to wrinkle and collapse

Results

Loss of the typical cellular structure of cork affected by yellow stain (observed via SEM and TEM)

SEM analysis of standard cork (SC) revealed a regular structure characterized by closed, prismatic cells, predominantly rectangular, arranged in a typical “honeycomb” pattern as previously reported [14] (Fig. 2a). Higher magnification observations disclosed the presence of microorganisms colonizing the cork within the cells (Fig. 2b).

Macroscopically, visual inspection of cork affected by the YS revealed pale yellow spots located immediately below the bark (Fig. 1). SEM observations at the cellular level indicated significant differences compared to standard cork. The YS-affected cork exhibited extensive structural damage, particularly evident on the left side of Fig. 2c, where cells appeared wrinkled and prone to collapse, disrupting the typical ordered cell structure seen in standard cork (right side of Fig. 2c). Additionally, the YS cork showed extensive microbial colonization, with a notable presence of filamentous fungi (Fig. 2d, e, f). The observation presented in Fig. 2d suggests that these microorganisms are capable of degrading the cork structure as they progress in their colonization. This results in the complete destruction of the typical cellular structure, as seen on the left side of Fig. 2d. In the vicinity of the advance zone, marked by the black dashed line, and extending to the right, the cells begin to collapse and wrinkle, as depicted on the right side of Fig. 2d.

A more detailed examination of the cell wall structure of phellem (cork) cells was conducted using TEM (Fig. 3).

Consistent with previous reports [70], the cell wall of suberized cork cells comprises four successive layers (Fig. 3a): the middle lamella, a very thin lignin-rich primary cell wall, a thick and highly suberized secondary cell wall, and a tertiary cell wall. Thin channels, approximately 50 nm in diameter, known as plasmodesmata (Fig. 3a, b), traverse the cell walls and function as intercellular channels, facilitating the transport of signalling molecules between living cells [70]. This regular structure was frequently disrupted in YS cells (Fig. 3b, c, d), with instances of complete disappearance of hemilayers of the tertiary and secondary cell walls (Fig. 3b).

Microbial structures were frequently observed attached to the cell wall in cork affected by YS (Fig. 3c, d). Cell wall exhibited severe damage, characterized by the disappearance of the tertiary wall and the disorganization and degradation of the secondary wall (Fig. 3c, d). Additionally, there were instances where the middle lamella and the secondary wall showed a tendency towards physical separation, with the secondary wall beginning to exhibit signs of degradation (Fig. 3d).

Overview of bacterial and fungal populations on cork

SEM data revealed abundant microbial colonization in cork affected by the YS. This observation was corroborated by quantifying the viable fungal and bacterial isolates in both SC- and YS-affected cork. The SC contained an average estimated value of 1.17×10^5 filamentous fungi/g of cork, whereas the cork affected by the YS contained a 4.39-fold increase, with populations of 5.13×10^5

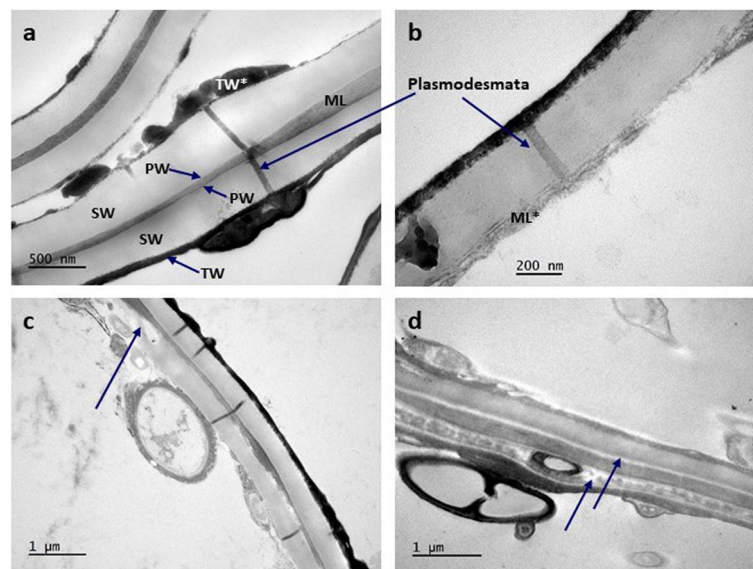


Fig. 3 Structure of cell walls observed by TEM in standard cork (**a**) and yellow stain (**b, c, d**). As shown in **a**, the cell wall comprises four successive layers: the middle lamella (ML), the primary wall (PW), which is a very thin layer adjacent to the ML (not evident), the highly suberized secondary wall (SW), and the tertiary wall (TW). Plasmodesmata traversing the cell wall are indicated by arrows in **a** and **b**. As it can be observed in **b**, some cells in YS exhibit a disorganized and discontinuous ML (ML*), with the removal of SW and TW; in **c**, there is TW removal, disorganization, and partial degradation of SW (indicated by an arrow). In **d**, separation between ML and SW, along with disorganization and partial degradation of SW, is observed (indicated by arrows) in YS cells. Microbial structures adjacent to the cell wall are visible in **c** and **d**

filamentous fungi/g of cork. In terms of the bacterial population, SC contained an average estimated value of 7.58×10^5 bacteria/g of cork, whereas the bacterial amount in YS was 4.16 times greater, reaching an average value of 3.15×10^6 bacteria/g of cork (Supplementary Fig. 1).

The bacterial and fungal communities of cork were analyzed via the Illumina MiSeq paired-end sequencing platform, which uses the ITS and 16S rRNA barcodes, respectively. The ITS rRNA amplicon samples analyzed for the fungal community generated 4,996,684 raw reads, with a mean of $499,668.4 \pm 179,444$ reads per sample. After filtering, 99% of them (average of $494,962.6 \pm 177,746$) were retained. A total of 4147 fungal ASVs were initially detected, of which 659 (15.89% of the total) were unidentified by matching in the UNITE database. After applying the quality filters, the dataset consisted of 1680 fungal ASVs taxonomically assigned to 5 different phyla, 23 classes, 78 orders, 178 families, and 270 genera (Supplementary Table 1). The dominant phyla in the fungal community were Ascomycota (representing 62.21% and 66.59% of the total ASVs in YS and SC, respectively) and Basidiomycota (27.38% and 32.73%, respectively). Notably, the phyla Mucoromycota (6.60% and 0.13% in YS and SC, respectively), Mortierellomycota (3.67% and 0.48% in YS and SC, respectively), and Chytridiomycota (0.14% and 0.07%, respectively) presented greater abundances in YS than in SC (Fig. 4a),

although the Wilcoxon test revealed no significant differences between these taxa for the two types of cork.

On the other hand, for the 16S rRNA amplicons (bacterial community), 8,114,466 raw sequences were generated for the 10 samples analyzed, with an average of $809,446 \pm 28,440$ reads per sample. After filtering, 99.3% ($805,801 \pm 285,424$ on average) of the reads were retained. The filtered 16S rRNA sequences were assigned to 35,394 bacterial ASVs. These sequences represented $76.39 \pm 2.82\%$ of the total sample composition, with the remaining being mitochondrial ($4.59 \pm 0.1\%$), chloroplast ($0.35 \pm 0.1\%$), and unclassified ($18.67 \pm 1.2\%$) sequences. After applying the quality filters, the bacterial dataset consisted of a total of 9715 ASVs taxonomically assigned to 26 phyla, 56 classes, 130 orders, 212 families, and 438 genera (Supplementary Table 2).

The dominant phyla in the bacterial community (Fig. 4d) were Proteobacteria (43.93% and 38.69% in YS and SC, respectively) and Actinobacteria (23.92% and 23.29% in YS and SC, respectively). YS was enriched in several phyla, such as Bacteroidota (8.24%), Acidobacteriota (7.07%), Verrucomicrobiota (3.44%), and Armatimonadota (0.73%), compared with SC, where their relative abundances were 2.7%, 2.8%, 1.3%, and 0.3%, respectively. In addition, several orders were relatively more abundant in YS than in SC, such as Acetobacteriales (2.33%), Chitinophagales (3.00%), Micrococcales (2.01%),

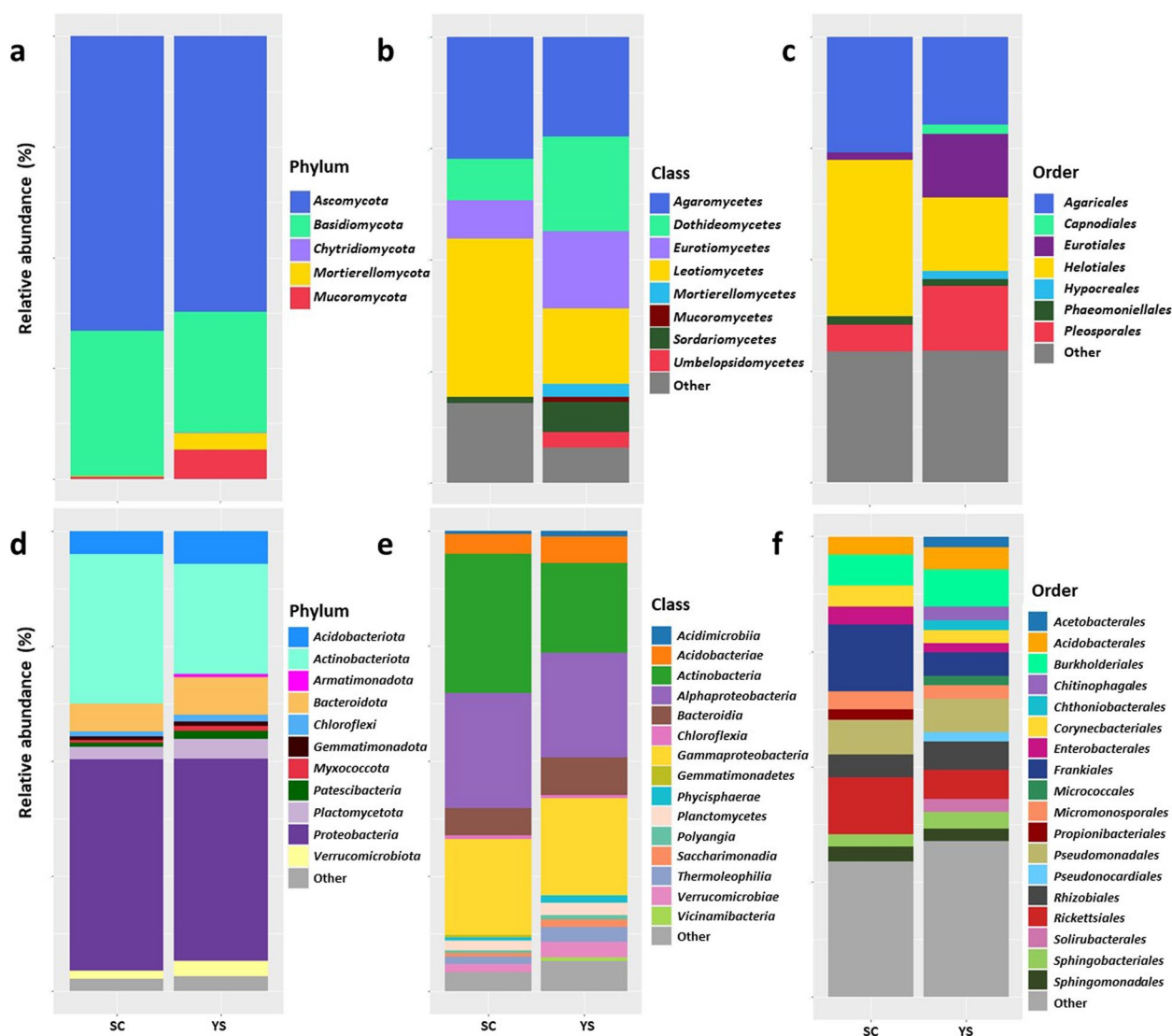


Fig. 4 Composition of cork microbial populations. Mean relative abundance distribution at phylum (a, d), class (b, e), and order (c, f) of fungal (a, b, c) and bacterial communities (d, e, f) in standard cork (SC) and yellow stain (YS). "Other" includes all taxa with a relative abundance of less than 2.0%

Pseudonocardiales (2.06%), and Solirubrobacteriales (2.93%), whose levels in SC were 1.59%, 1.62%, 1.07%, 1.59%, and 1.54%, respectively. In contrast, members of the order Propionibacteriales were more abundant in SC (2.30%) than in YS (1.00%) (Fig. 4f). All these differences in bacterial abundance were statistically significant.

Analysis of the α - and β -diversity of microbial communities

Different classical ecological indices (Chao1, Shannon, Gini-Simpson, and Pielou) were calculated to assess the α -diversity of the microbial communities in both the YS and SC samples. α -Diversity represents the variety and distribution of species within a community. The Chao1 index estimates species richness, approximating the total

number of unique species present. The Shannon index combines richness and evenness, reflecting the probability that two randomly selected individuals from the dataset belong to different species. Similarly, the Gini-Simpson (1-D) index measures the probability that two individuals randomly chosen do not belong to the same species, while the Pielou index focuses specifically on the evenness of the species distribution. Overall, both the variety of species (diversity) and the even distribution of individuals among these ASVs (evenness) were found to be high in both the fungal (Fig. 5a) and bacterial (Fig. 5b) communities. Shannon index values above 3.5 indicate considerable microbial diversity, whereas the Gini-Simpson (1-D) and Pielou indices, with values very close to 1,

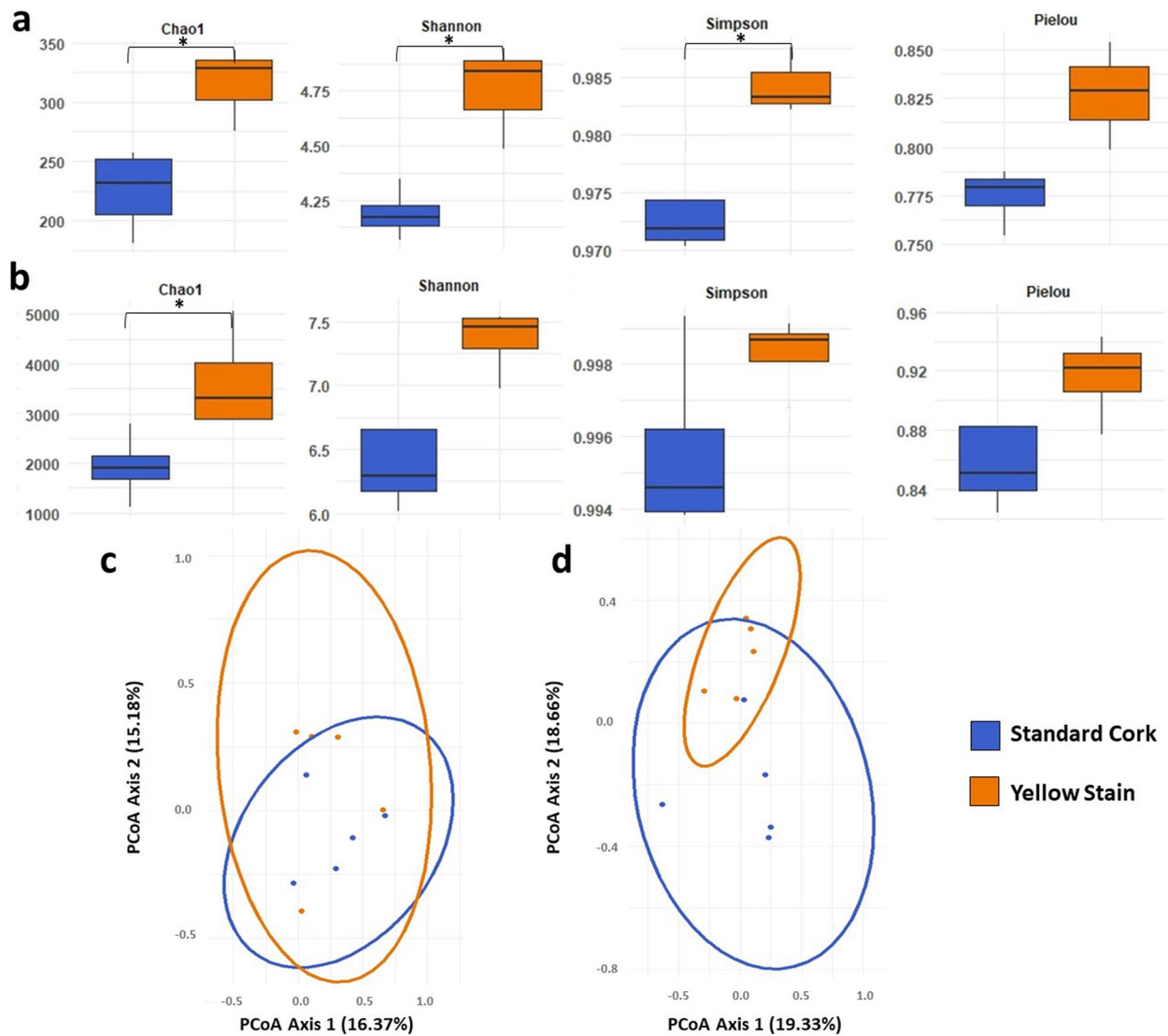


Fig. 5 Analysis of the diversity of microbial populations in cork. *a*- and β -diversity of fungal (**a**, **c**) and bacterial (**b**, **d**) communities in standard cork and cork affected by yellow stain. Box plots of Chao1, Shannon, Simpson-Gini, and Pielou's evenness indices are shown in **a** and **b**, where the asterisk indicates significant differences (p -value < 0.05) after performing a Wilcoxon test. PCoA analysis based on Bray–Curtis distances in the fungal and bacterial communities is shown in **c** and **d**, respectively, with ellipses indicating the 95% confidence interval

further confirmed high diversity and low single-species dominance, implying a very even species distribution [71–73]. Based on these data, the analyzed cork samples appeared to host diverse and well-balanced microbial communities, with no significant dominance by a few ASVs. In particular, significant differences in α -diversity were observed between the YS and SC samples for fungal communities, except for Pielou's evenness index (Fig. 5a) (Supplementary Table 3). In contrast, only the Chao1 index was significantly different when the α -diversity of the bacterial community was analyzed (Fig. 5b) (Supplementary Table 4). Although the remaining indices did

not significantly differ, the diversity and evenness metrics were consistently greater in the YS samples than in the SC samples.

A PCoA based on the Bray–Curtis dissimilarity matrix was performed to explore the β -diversity of the microbial communities between the YS and SC samples (Fig. 5c, d). β -Diversity refers to differences in microbial community composition across sample groups. The Bray–Curtis dissimilarity matrix quantifies these differences by comparing the presence, abundance, and composition of ASVs among samples. The PCoA plot revealed no distinct clustering or separation between the YS and SC samples,

suggesting substantial overlap in microbial community composition. PERMANOVA was performed to assess these dissimilarities statistically. The test indicated no significant differences in the fungal communities between the YS and SC samples ($R^2=0.11$, p -value=0.497). However, slightly significant dissimilarities were observed in the bacterial communities ($R^2=0.14$, p -value=0.03). These results suggest that while fungal communities are similar between YS and SC, bacterial communities exhibit some differences. Overall, the findings imply that both types of cork samples may share similar ecological niches or display comparable responses to environmental factors.

Differential abundances at the genus/species level when comparing standard cork and yellow stain

DESeq2 was used to identify differences in taxon abundance between the YS and SC cork samples at the genus or species level. In the fungal community, 26 ASVs were found to have significantly different abundances (p -value<0.01) between the YS and SC samples (Supplementary Table 5). All of them presented an $LFC>0$, indicating that their abundance increased in YS cork compared with SC cork and belonged to the phyla Ascomycota, Mucoromycota, and Mortierellomycota. Among these ASVs, there was a predominance of *Penicillium* (six ASVs), *Umbelopsis* (six ASVs), *Mucor* (three ASVs), and *Mortierella elongata* (two ASVs), and one ASV each belonging to the genera *Absidia*, *Geomyces*, *Metapochonia*, *Pseudogymnoascus*, and *Talaromyces*, while one ASV was identified as *Entomortierella lignicola*, and three ASVs were unclassified isolates at the genus/species level. Among these, members of *Mortierella* [74], *Mucor* [75], *Penicillium* [76–78], and *Umbelopsis* [79] have been reported as lignin degraders in several studies.

In the bacterial community, 26 ASVs with significantly different abundances were detected between the YS and SC samples (Supplementary Table 6). A total of 14 bacterial ASVs presented an $LFC>0$; therefore, their abundance was greater in the YS than in the standard cork. All these ASVs, with the exception of one belonging to the phylum Planctomycetota, belong to Proteobacteria. Among them, there was a predominance of Burkholderiales (7 ASVs), which more specifically belong to the *Burkholderia-Caballeronia-Paraburkholderia* group, and Enterobacterales (5 ASVs). The *Burkholderia-Caballeronia-Paraburkholderia* group is a complex group of closely related species, all of which were initially included in the genus *Burkholderia*. However, recent taxonomic studies have reclassified all these species into *Burkholderia*, a genus that retains this name and consists mainly of animal and plant pathogens, and the genera *Paraburkholderia* and *Caballeronia*, which contain mainly the

so-called environmental bacteria [80]. Members of these groups are well known for their high ability to metabolize aromatic compounds, which are particularly abundant in the guts of xylophagous insects and wood litter [81]. Enterobacterales is known to include some species involved in lignin degradation, such as *Klebsiella* sp. [81], *Klebsiella aerogenes* [82], *Klebsiella pneumoniae* [83], *Enterobacter lignolyticus* [84], *Serratia* sp., and *Serratia liquefaciens* [85]. Recently, it has been reported that winter warming in Alaska accelerates lignin decomposition by Proteobacteria, with 95.1% of the total abundance of potential lignin decomposers belonging to the genus *Burkholderia* [86].

Isolation and characterization of filamentous fungi from cork and their putative role in suberin/lignin biodegradation

A total of 386 fungal isolates were obtained from SC (137 isolates) and YS (249 isolates) by using different microbiological agar media (RB, PDA, and MEA). After isolation, they were replicated on PDA and classified into 51 different isolates according to macroscopic (mycelium colour, sporulation, pigment, or exudate production) and microscopic (observation of mycelial and spore-forming structures) characteristics, which were later identified at the genus level by sequencing the ITS rRNA region (Supplementary Table 7). Most of the isolates (41) were Ascomycota belonging to the genera *Alternaria*, *Aspergillus*, *Chaetomium*, *Cladosporium*, *Coniella*, *Coniochaeta*, *Cryphonectria*, *Cytospora*, *Epicoccum*, *Fusarium*, *Neocucurbitaria*, *Paraconiothyrium*, *Penicillium*, *Pyrenophora*, *Talaromyces*, *Trichocladium*, and *Trichoderma*. Mucoromycota were represented by *Absidia*, *Entomortierella*, *Linnemannia*, *Mortierella*, *Mucor*, and *Umbelopsis* (nine isolates), whereas only one representative of Basidiomycota was detected, belonging to the genus *Coprinellus* (Fig. 6). As shown in Fig. 6, the most represented genus was *Penicillium*, with a total of 10 isolates, followed by *Trichoderma* (6 isolates), *Fusarium* and *Talaromyces* (4 isolates each), and *Umbelopsis* (3 isolates). A total of 10 isolates were detected in both the standard cork and YS samples, whereas 16 were solely isolated from standard cork, and 25 were isolated from the YS only (Fig. 6). Most of the fungal isolates presented some traits related to lignin degradation. Thus, 42 out of the 51 different isolates (82.35%) were able to grow in minimal medium containing Kraft lignin as the sole carbon source, indicating the ability to metabolize and/or degrade this lignin compound (Table 1). The ability of 60.78% of the fungal isolates (31 out of 51) to oxidize ABTS, a trait associated with the production of laccases, was clear. Fifteen of the 51 isolates (29.41%) were able to completely discolor the RB5 and RBBR dyes, an aspect directly related to the

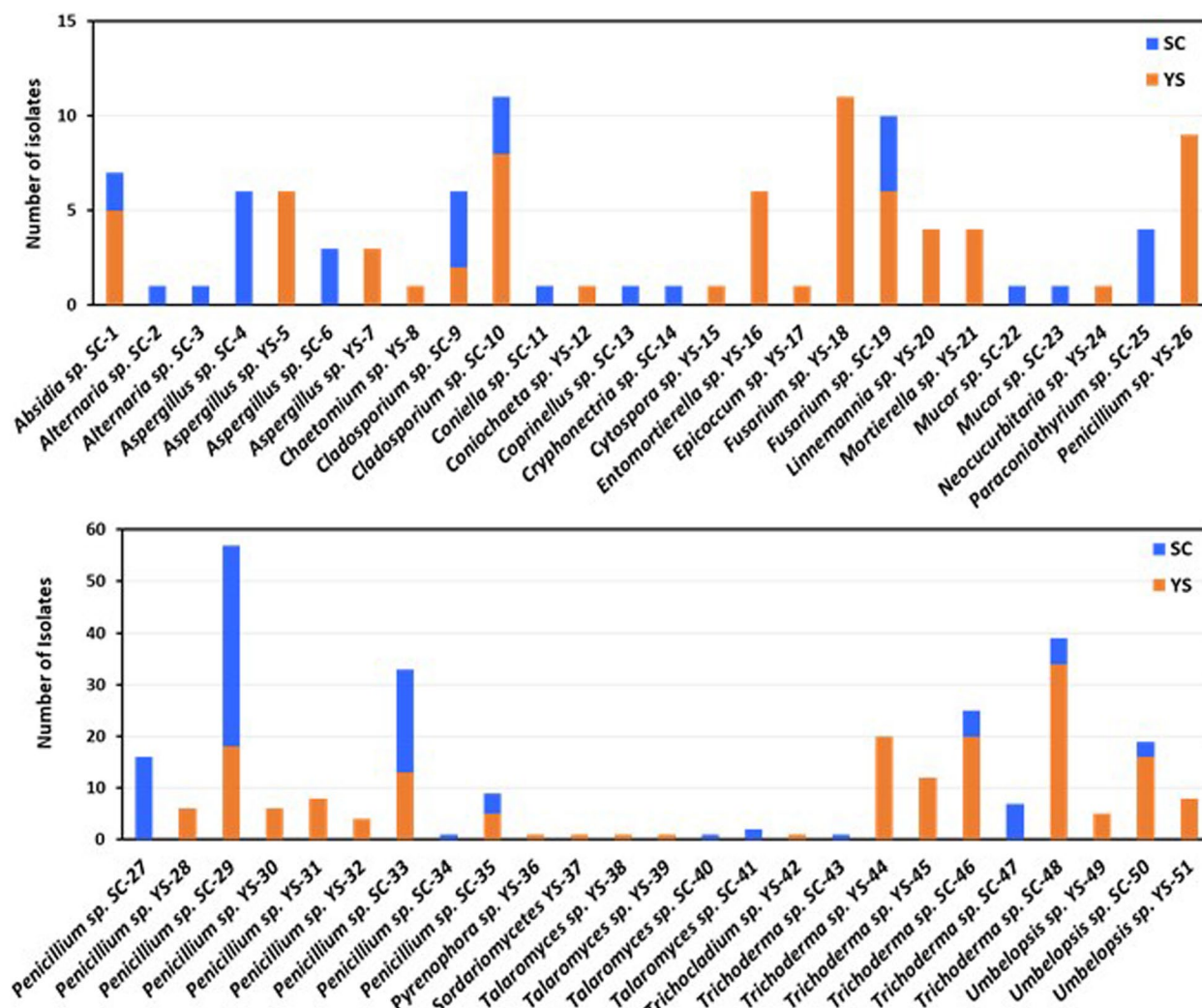


Fig. 6 Fungal isolates identified to genus level isolated from standard cork (SC) and yellow stain (YS)

ability to produce some type of peroxidase related to lignin degradation, such as LiP, MnP, or VP. In contrast, 54.90% of the isolates (28 out of 51) were able to completely discolor one of the two dyes, or partially discolor both (Table 1).

CPO activity was also detected in 70.59% of the fungal isolates tested, as they were able to oxidize phenol in the presence of chloride and hydrogen peroxide, as tested in enzyme assays carried out with culture supernatants.

Indeed, an *in silico* analysis of the UniProt database to detect the presence of CPO enzymes in fungi and bacteria revealed the existence of CPO enzymes in many bacterial and fungal taxa (Supplementary Table 8). A total of 8078 hits were identified as putative CPOs, of which 96.61% (7804 protein sequences) corresponded to heme-dependent CPOs. Within this protein group, only the fungal kingdom was represented, belonging to

six different phyla. As expected, the most abundant phylum was Ascomycota (66.73% of the detected protein sequences), followed by Basidiomycota (31.52%) and, to a lesser extent, Mucoromycota (1.22%), Chytridiomycota (29 sequences; 0.37%), Zoopagomycota (10 sequences; 0.13%), and Cryptomycota (2 protein sequences; 0.03%). On the other hand, 274 hits corresponding to vanadium-dependent CPOs were detected. Of these, 92 of the protein sequences (33.58%) belonged to the fungal kingdom, all within the phylum Ascomycota. The remaining proteins belonged to Bacteria and were distributed across 18 phyla, with Cyanobacteriota (56 protein sequences, 30.77%), Actinomycetota (19.78%), and Pseudomonadota (15.93%) being the most representative. These findings confirmed the data described above by detecting CPO activity in the fungal strains isolated from our cork samples, confirming that CPO activity is widely distributed

Table 1 Traits related to lignin biodegradation and chloroperoxidase (CPO) activity in fungal isolates of cork

Isolate	ABTS ^a	RB5 ^{a,b}	RBBR ^{a,b}	Growth on kraft lignin ^a	CPO
<i>Absidia</i> sp. SC1	+	+	+	+	+
<i>Alternaria</i> sp. SC2	-	+	±	+	+
<i>Alternaria</i> sp. SC3	+	±	±	+	+
<i>Aspergillus</i> sp. SC-4	-	+	+	+	+
<i>Aspergillus</i> sp. YS-5	-	+	±	+	+
<i>Aspergillus</i> sp. SC-6	+	±	±	+	+
<i>Aspergillus</i> sp. YS-7	+	±	±	+	+
<i>Chaetomium</i> sp. YS-8	+	+	±	+	+
<i>Cladosporium</i> sp. SC-9	+	+	±	+	+
<i>Cladosporium</i> sp. SC-10	+	+	+	+	+
<i>Coniella</i> sp. SC-11	+	±	±	-	+
<i>Coniochaeta</i> sp. YS-12	+	±	±	-	+
<i>Coprinellus</i> sp. SC-13	+	±	±	+	+
<i>Cryphonectria</i> sp. SC-14	+	±	±	-	-
<i>Cytospora</i> sp. YS-15	+	±	±	-	+
<i>Entomortierella</i> sp. YS-16	-	+	±	+	+
<i>Epicoccum</i> sp. YS-17	-	-	-	-	-
<i>Fusarium</i> sp. YS-18	+	+	+	+	+
<i>Fusarium</i> sp. SC-19	+	+	+	+	+
<i>Linnemannia</i> sp. YS-20	+	+	±	-	-
<i>Mortierella</i> sp. YS-21	-	±	±	+	+
<i>Mucor</i> sp. SC-22	-	-	-	+	-
<i>Mucor</i> sp. SC-23	+	+	+	+	+
<i>Neocucurbitaria</i> sp. YS-24	+	+	+	+	+
<i>Paraconiothyrium</i> sp. SC-25	+	-	-	+	-
<i>Penicillium</i> sp. YS-26	+	±	-	+	-
<i>Penicillium</i> sp. SC-27	-	±	±	+	-
<i>Penicillium</i> sp. YS-28	-	+	±	+	-
<i>Penicillium</i> sp. SC-29	-	-	-	+	-
<i>Penicillium</i> sp. YS-30	+	±	±	+	-
<i>Penicillium</i> sp. YS-31	+	±	±	-	-
<i>Penicillium</i> sp. YS-32	+	+	+	+	-
<i>Penicillium</i> sp. SC-33	+	±	±	+	-
<i>Penicillium</i> sp. SC-34	+	-	+	+	-
<i>Penicillium</i> sp. SC-35	+	±	±	+	-
<i>Pyrenophora</i> sp. YS-36	+	±	±	+	+
<i>Sordariomycetes</i> YS-37	-	-	-	+	+
<i>Talaromyces</i> sp. YS-38	+	±	±	+	+
<i>Talaromyces</i> sp. YS-39	-	-	-	+	+
<i>Talaromyces</i> sp. SC-40	+	±	±	+	+
<i>Talaromyces</i> sp. SC-41	+	±	±	+	+
<i>Trichocladium</i> sp. YS-42	+	+	+	+	+
<i>Trichoderma</i> sp. SC-43	-	±	±	+	+
<i>Trichoderma</i> sp. YS-44	+	+	+	+	+
<i>Trichoderma</i> sp. YS-45	-	±	±	+	+
<i>Trichoderma</i> sp. SC-46	+	±	±	+	+
<i>Trichoderma</i> sp. SC-47	-	+	+	+	+
<i>Trichoderma</i> sp. SC-48	+	+	+	+	+
<i>Umbelopsis</i> sp. YS-49	+	±	±	-	+
<i>Umbelopsis</i> sp. SC-50	+	+	+	+	+
<i>Umbelopsis</i> sp. YS-51	-	+	+	-	+

^a ABTS oxidation, discoloration of RB5 and RBBR, and growth on kraft lignin were observed at 14 days of growth

^b For the assays with RBBR and RB5 dyes, a “+” sign indicates a total discolouration of the dye on the plate, while the “+/-” sign refers to the detection of partial discolouration around the fungal colony

among fungal taxa. In fact, CPOs were detected in the UniProt database in all of the genera of fungi isolated from our cork samples which are listed in Fig. 6.

Extractable aromatic compounds present in cork

The compounds from five cork samples were extracted via a basic solution and concentrated prior to LC–MS analysis via solid-phase extraction (SPE). More than 14,500 features were detected in the chromatograms of the extracts. Their measured m/z values were compared with the theoretical m/z values of different phenolic compounds (Supplementary Table 9), and 130 coincidences were found (Supplementary Table 10). Finally, 11 compounds were identified via comparison of their MS/MS spectra, and/or with chemical standards, as shown in Table 2. All the compounds listed in Table 2 were previously reported in the literature to be present in cork samples or to be produced by lignin degradation [7, 87–89].

The first compound (*p*-hydroxybenzoic acid) was a mixture of two isomers because two different MS/MS spectra (Supplementary Fig. 3) could be obtained along the peak from the same precursor m/z (137.02448). One of them, *p*-hydroxybenzoic acid was confirmed with the injection of the pure standard, resulting in the same retention time and MS/MS spectra. Some possibilities for the other isomer were studied among compounds previously reported in the literature, but salicylic acid did not have the same retention time, and the MS/MS spectra of gentisate aldehyde and protocatechualdehyde (2,5/3,4-dihydroxybenzaldehyde) did not match. Some similarities with the MS/MS spectra of 2,5-dihydroxybenzaldehyde (Supplementary Fig. 3) were found, although they were not sufficient to confirm the annotation. This mixture of isomers shows the most intense

signal, followed by ferulic acid, *p*-coumaric acid, and esculetin (Table 2).

Isolation of vanillic acid-catabolizing bacteria and the production of phenol from *p*-hydroxybenzoic acid in a resting cell system

As mentioned above, two of the aromatic compounds detected in cork caught our attention, *p*-hydroxybenzoic acid and phenol, as they could be putative precursors for the production of CPs. It has been previously reported that *p*-hydroxybenzoic acid can be produced from lignin breakdown [7]. Indeed, depolymerization of lignin produces *p*-hydroxyphenyl units that are later converted to *p*-hydroxybenzoate [6]. It has been reported that some bacteria, such as *Enterobacter cloacae* P240 [90] and *Bacillus subtilis* ATCC 6051 [91], possess a *p*-hydroxybenzoate decarboxylase activity. The case of *B. subtilis* was particularly interesting since it was reported to be able to decarboxylate vanillate and *p*-hydroxybenzoate, under both anaerobic and aerobic conditions, to produce guaiacol and phenol, respectively. In fact, cultures of these bacteria supplemented with 5-mM *p*-hydroxybenzoate were capable of decarboxylating 95% of this compound to phenol [91]. This study suggested that a single enzyme could decarboxylate vanillate and *p*-hydroxybenzoate. In a previous work, we isolated several bacterial strains from cork samples, including one *B. subtilis* strain and three strains of the genus *Streptomyces*, which were able to efficiently decarboxylate vanillate to guaiacol, as a result of a vanillate decarboxylase activity [39].

With this prior information, we decided to isolate different types of Bacteria (enterobacteria, spore-forming bacilli, and actinobacteria) from YS samples in a minimal medium with vanillate as the sole carbon source. A total

Table 2 Phenolic compounds identified in extracts of cork samples affected by YS analyzed by UHPLC–MS/MS (ESI[−])

Compound	Measured m/z	RT (min)	Molecular formula	Name	Intensity ^a	PubChem CID
1	137.02448	6.26	C ₇ H ₆ O ₃	# <i>p</i> -Hydroxybenzoic acid ¹	2,777,727 ± 331,481	135
2	177.01926	6.93	C ₉ H ₆ O ₄	Esculetin ²	1,281,014 ± 186,217	5,281,416
3	179.03488	6.98	C ₉ H ₈ O ₄	Caffeic acid ¹	169,245 ± 17,163	689,043
4	165.05585	7.41	C ₉ H ₁₀ O ₃	Homovanillin ²	50,011 ± 5890	151,276
5	163.04011	7.68	C ₉ H ₈ O ₃	<i>p</i> -Coumaric acid ¹	1,169,958 ± 183,394	637,542
6	93.03468	7.68	C ₆ H ₆ O	Phenol ¹	46,629 ± 6793	996
7	151.04018	7.69	C ₈ H ₈ O ₃	Vanillin ¹	434,919 ± 47,457	1183
8	193.05035	7.97	C ₁₀ H ₁₀ O ₄	Ferulic acid ¹	1,823,292 ± 179,736	445,858
9	147.0454	8.29	C ₇ H ₆ O ₃	<i>p</i> -Coumaraldehyde ²	348,924 ± 6178	641,301
10	177.05563	8.52	C ₉ H ₆ O ₄	Coniferyl aldehyde ²	117,266 ± 6596	5,280,536

[#] The peak corresponding to *p*-hydroxybenzoic acid was a mix of two isomers

^a Mean of intensity of five samples. A boxplot graphic for each compound is shown in Supplementary Fig. 2

^{1,2} Superscript numbers indicate annotation level following rules described by Sumner et al. [106]

of 17 bacterial isolates were identified for their ability to decarboxylate vanillate, including 4 isolates belonging to the genus *Burkholderia-Caballeronia-Paraburkholderia*, 1 to the genus *Novosphingobium*, 2 to the genus *Stenotrophomonas*, 7 isolates belonging to the genus *Pseudomonas*, 2 isolates to the genus *Streptomyces*, and 1 isolate belonging to the genus *Variovorax* (Supplementary Table 11). To test whether these bacterial isolates were also capable of decarboxylating *p*-hydroxybenzoate, resting cell systems supplemented with this compound were used. Among all the isolates tested, only two strains (YS-B37 and YS-A2) belonging to the genus *Streptomyces* were able to produce phenol from *p*-hydroxybenzoate (Fig. 7).

Phenol accumulation in the resting cell supernatant was observed in both strains after 8 h. In strain YS-A2, the concentration of *p*-hydroxybenzoate decreased from an initial 12 to 4.18 mM after 48 h of incubation, indicating a reduction of 65.17%. The maximum phenol concentration was recorded at 24 h, reaching 77.56 µg/mL, and decreased slightly to 72.93 µg/mL by the end of the experiment (Fig. 7). This indicates that 6.83% of the *p*-hydroxybenzoate is excreted as phenol in the supernatant of the resting cell. Conversely, strain YS-B37 exhibited greater biotransformation efficiency, with the initial *p*-hydroxybenzoate concentration being completely depleted after 48 h of incubation, and the corresponding excreted phenol level reaching 30.42% (Fig. 7).

Both strains were also able to grow in a minimal medium containing *p*-hydroxybenzoate as the sole carbon source. However, the growth rate of strain YS-B37 was significantly higher than that of the other strains, indicating a superior capacity for *p*-hydroxybenzoate assimilation. Consequently, this study reveals that

bacteria capable of biotransforming *p*-hydroxybenzoate into phenol can be isolated from cork samples, particularly from YS samples.

The formation of chlorophenols and chloroanisoles is mediated by chloroperoxidase activity

Following the successful demonstration of phenol production from *p*-hydroxybenzoate, it was hypothesized that CPs, including 2,4,6-TCP, could be synthesized from phenol through a reaction catalyzed by a CPO enzyme. CPO enzymes facilitate hydrogen peroxide (H₂O₂)-dependent halogenation reactions, primarily chlorination, and to a lesser extent, iodination and bromination, across a diverse range of substrates. It has been proposed that fungal CPOs can oxidize chloride ions to hypochlorous acid [92]. Recent studies have reported that CPO from *C. fumago* can efficiently brominate phenol, yielding compounds such as 4-bromophenol (4-BP), 2,4-dibromophenol (2,4-DBP), and 2,4,6-tribromophenol (2,4,6-TBP) [69]. Additionally, in silico analysis confirmed the presence of CPO proteins in a wide array of filamentous fungi and bacteria (Supplementary Table 8), encompassing all genera identified in the cork samples analyzed in this study. Notably, a significant proportion of fungal isolates from the cork samples exhibited CPO activity, as evidenced by assays conducted on culture supernatants (Table 1).

Building on this knowledge, we aimed to investigate whether CPO from *C. fumago* could catalyze the chlorination of phenol and/or anisole to produce CPs and CAs, respectively (Fig. 8).

In vitro confirmed that CPO could chlorinate phenol to produce 2-CP, 4-CP, 2,4-DCP, and 2,4,6-TCP,

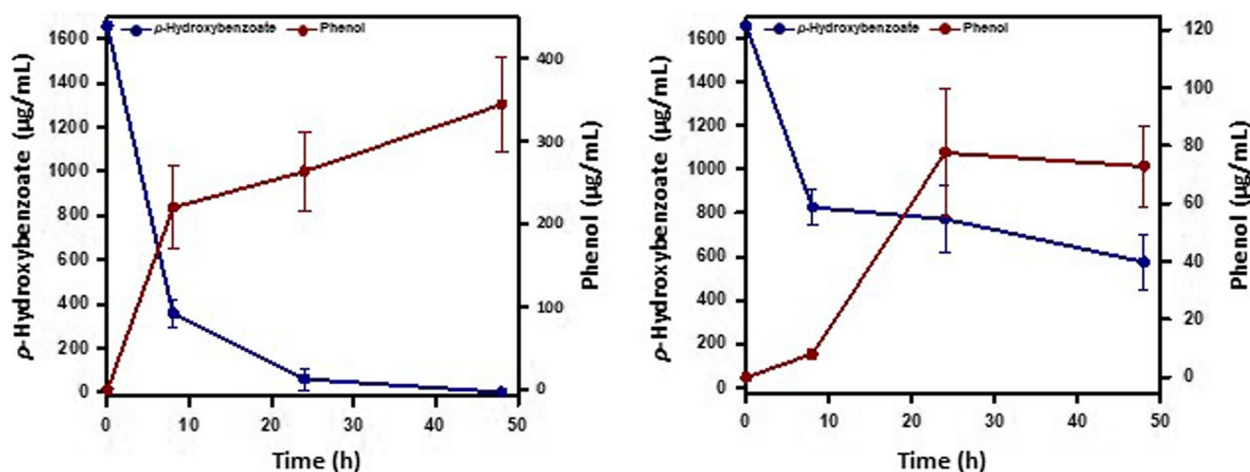


Fig. 7 Bioconversion of *p*-hydroxybenzoate to phenol in resting cell systems of bacterial isolates *Streptomyces* sp. YS-B37 (left) and *Streptomyces* sp. YS-A2 (right). Data shown are the average of three independent experiments made by duplicate

with yields of 40.7%, 11.4%, 4.9%, and 8.9%, respectively. Chlorination of 2-CP resulted in the formation of 2,4-DCP (24.2% conversion rate), 2,6-DCP (31.8%), and 2,4,6-TCP (17.4%). Similarly, the chlorination of 4-CP produced 2,4-DCP (7.5% conversion rate), 2,4,6-TCP (18.4%), and 2,3,4,6-TeCP (20.2%). When 2,4-DCP was used as the substrate, 2,4,6-TCP and 2,3,4,6-TeCP were formed, with conversion rates of 13.5% and 26.0%, respectively. No chlorinated products were detected when 2,6-DCP was used as a substrate. CPO exhibited halogenation activity on anisole, primarily converting it to 2-chloroanisole (2-CA) (55.6% conversion rate) and 4-chloroanisole (4-CA) (26.9%) (Fig. 8). These results indicate a preference for chlorination at the *ortho* position over the *para* position. No halogenation activity was observed when 2-CA, 4-CA, 2,4-dichloroanisole (2,4-DCA), and 2,6-dichloroanisole (2,6-DCA) were used as substrates. These findings clearly confirm that 2,4,6-TCP can be produced in cork due to the prevalent CPO activity of cork-dwelling fungal and/or bacterial strains, preferably using phenol and other mono- and dichlorophenols as substrates.

Discussion

YS is an alteration of cork tissue, characterized by a yellowish discoloration and a characteristic musty odor, attributed to elevated levels of 2,4,6-trichloroanisole (TCA) compared to the surrounding normal cork tissue. This defect frequently necessitates the disposal of affected cork planks, resulting in substantial economic losses for the cork stopper industry [1, 42]. Despite its impact, YS remains poorly understood, particularly concerning its high TCA content and microbiological characterization. YS is believed to result from an alteration of cork caused by *Armillaria mellea* (Vahl. Ex Fr.), a saprophytic basidiomycete that thrives on soil and lignocellulosic materials [93]. However, there is a lack of scientific or experimental evidence in the literature to support this claim. It has also been suggested that YS arises from a microbial attack capable of altering the cork structure. Some SEM studies have confirmed that cork affected by YS exhibits deformed, wrinkled cells with cell wall separation at the middle lamella level [14]. Both SEM and TEM analyses were conducted to verify this finding. SEM revealed that cork affected by YS exhibited a highly altered cellular structure, making it challenging to identify areas

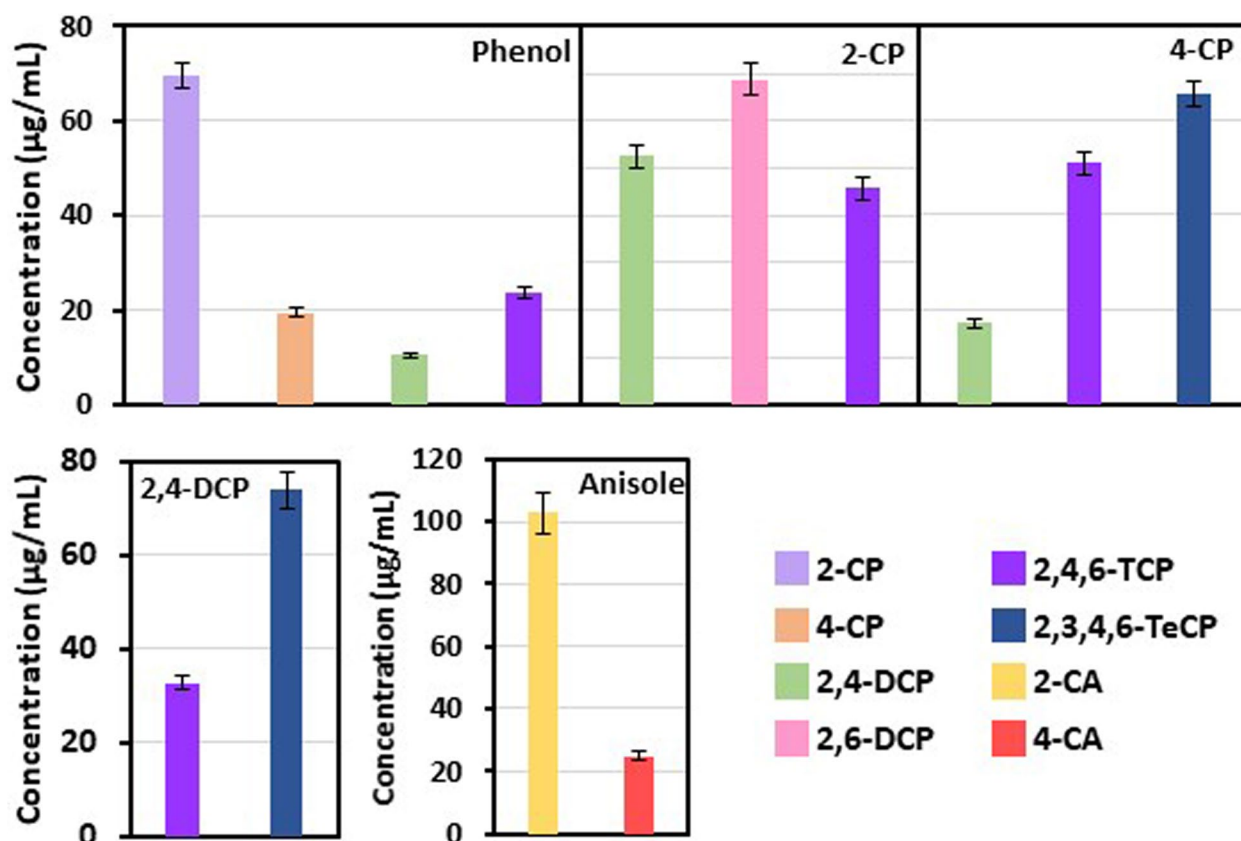


Fig. 8 Chloroperoxidase mediated chlorination of phenol and different chlorophenols in the presence of chloride and H₂O₂. Data shown are the average of three independent experiments made by duplicate

with the typical regular arrangement of polygonal cells observed in SC samples. Another notable observation was the extensive microbial colonization in YS, particularly by filamentous fungi, which are rarely seen in SC. TEM studies corroborated these findings, showing profound alterations in the cell wall structure, often resulting in a disorganized and discontinuous middle lamella, with partial or complete removal of the secondary and/or tertiary wall. These data unequivocally demonstrate that YS is associated with substantial structural alterations in cork, likely attributable to extensive microbial colonization and the resultant biodegradation activity.

SEM analyses revealed profuse microbial colonization in cork samples affected by YS, a finding corroborated by classical microbial isolation data. Specifically, YS exhibited, on average, 4.39 and 4.16 times greater fungal and bacterial populations, respectively (Supplementary Fig. 1). These microbial populations were further analyzed through metataxonomic analysis, enabling a comparative assessment. The fungal community was dominated by Ascomycota and Basidiomycota, whereas at the class level, the most abundant taxa were Leotiomycetes, Agaricomycetes, Dothideomycetes, Eurotiomycetes, and Sordariomycetes. A similar composition at the phylum and class levels has been reported for grapevine wood [94], although in this case the relative abundances of the dominant taxa at the class level were Dothideomycetes (46.2%), Sordariomycetes (21.8%), Eurotiomycetes (13.0%), Agaricomycetes (8.1%), Leotiomycetes (4.6%), and Lecanoromycetes (2.0%). An enrichment in YS (significant differential abundance) was detected for 26 fungal ASVs belonging to *Penicillium* (6 ASVs), *Umbelopsis* (6 ASVs), *Mucor* (3 ASVs), and *Mortierella* (2 ASVs), which were the most significant. Interestingly, some of these taxa that were more abundant in the YS could be involved in lignin degradation. The cork contains an average of 22.0% lignin [4] or at least an equivalent polyaromatic fraction [9]. Therefore, it is not unreasonable to assume that microorganisms with the ability to degrade lignin could be involved in the degradation of the aromatic component of cork. *Penicillium* sp. and *Umbelopsis* isolates were the most represented among these significantly differentially abundant ASVs detected in the YS. Interestingly, some *Penicillium* isolates are lignin degraders [81], such as *Penicillium chrysogenum* [76, 95], *Penicillium simplicissimum* [78], and *Penicillium decumbens* [77]. *Umbelopsis isabellina* (ASV521 being more abundant in YS) has been reported to cause decay in *Quercus mongolica*, and this decay has been linked to the production of laccases involved in lignin degradation [79]. Recently, a strain of the genus *Mucor* was isolated from long-decayed wood and identified as a lignin degrader based on its high laccase activity [75]. Isolates belonging

the genus *Mortierella* were found in all four different lignin-degrading microbial consortia isolated from wooden antiques, suggesting that this fungus could be involved in the degradation of lignin or lignin-like structures [74]. These data suggest that YS harbors relatively high populations of fungi capable of degrading lignin and presumably the aromatic fraction of suberin, potentially contributing to the extensive degradation of the cork structure observed in YS. The saprophytic fungal microbiota of cork appears to be rich in filamentous fungi with the capacity to metabolize and/or degrade lignin. This was confirmed by the isolation of fungi from cork, 82.35% of which were able to grow in minimal medium containing Kraft lignin as the sole carbon source. Furthermore, many of these isolates possess enzymes involved in lignin degradation, such as laccases (60.78% exhibited this activity) and peroxidases, as evidenced by their ability to decolorize the RB5 and RBBR dyes.

Regarding the bacterial community in cork, the dominant phyla were Proteobacteria and Actinobacteria. Several ASVs exhibited significantly different abundances when comparing SC and YS, with 14 bacterial ASVs being significantly more abundant in YS than in SC. Most of these ASVs belong to bacterial groups such as the *Burkholderia-Caballeronia-Paraburkholderia* group (seven ASVs) and Enterobacterales (five ASVs), which include different isolates or species identified as lignin degraders [81]. Members of the *Burkholderia-Caballeronia-Paraburkholderia* group stand out for having a variety of aromatic catabolic pathways involved in the further degradation of the aromatic compounds generated from lignin breakdown [96, 97]. It has also recently been reported that winter warming in Alaska accelerates the decomposition of lignin present in permafrost, and that isolates from the genus *Burkholderia* account for 95.1% of the total abundance of potential lignin decomposers [86]. Whether these bacteria are involved in lignin/suberin degradation, or simply metabolize aromatic compounds produced by other lignin/suberin decomposers (such as filamentous fungi), remains to be clarified.

YS has a different percentage of phenolic compounds than SC does [98] and contains higher amounts of 2,4,6-TCA [1, 42]. This fact is intriguing, as it could suggest that 2,4,6-TCA could be synthesized de novo in YS via several previously unknown processes. The analysis of extractable aromatic compounds from cork allowed us to detect two compounds that caught our attention: *p*-hydroxybenzoate and phenol. The detection of phenol was very interesting because it could be the starting point for the synthesis of 2,4,6-TCP, the direct precursor for the synthesis of 2,4,6-TCA by *O*-methylation. While the origin of the *p*-hydroxybenzoate detected in cork can be easily explained by the *p*-hydroxyphenyl units obtained

from the breakdown of the lignin present in cork, which are further converted into *p*-hydroxybenzoate [6] (see Fig. 9 for a summary of the described process by which 2,4,6-TCA would be formed de novo in cork, more abundantly in YS), the origin of the phenol detected in cork was not as obvious.

However, a review of the previous literature revealed that some bacteria are able to catalyze the non-oxidative decarboxylation of *p*-hydroxybenzoate to produce phenol, and this activity was previously reported in *E. cloacae* P240 [90] and *B. subtilis* ATCC 6051 [91]. Interestingly, the enzyme of this latter strain was also able to efficiently decarboxylate vanillate [91]. The isolation from the YS of two strains of the genus *Streptomyces* capable of converting *p*-hydroxybenzoate to phenol (Fig. 9) allowed

us to elucidate a possible mechanism for the formation of the latter compound. The different conversion rates of the YS-B37 and YS-A2 strains suggest that both strains may use alternative metabolic pathways, possibly including the protocatechuate and catechol pathways, leading to the TCA cycle via the β -ketoacid pathway or protocatechuate meta-cleavage pathway [99, 100], although the observed differences could be simply a consequence of their different abilities to metabolize *p*-hydroxybenzoate.

However, the direct precursor of 2,4,6-TCA is the pesticide 2,4,6-TCP, and the mechanism of its formation in YS remains to be elucidated. Chloroperoxidases (CPOs), a type of haloperoxidases, are involved in the chlorination of organic materials [92, 101] and lignin [102]. These enzymes are found in numerous

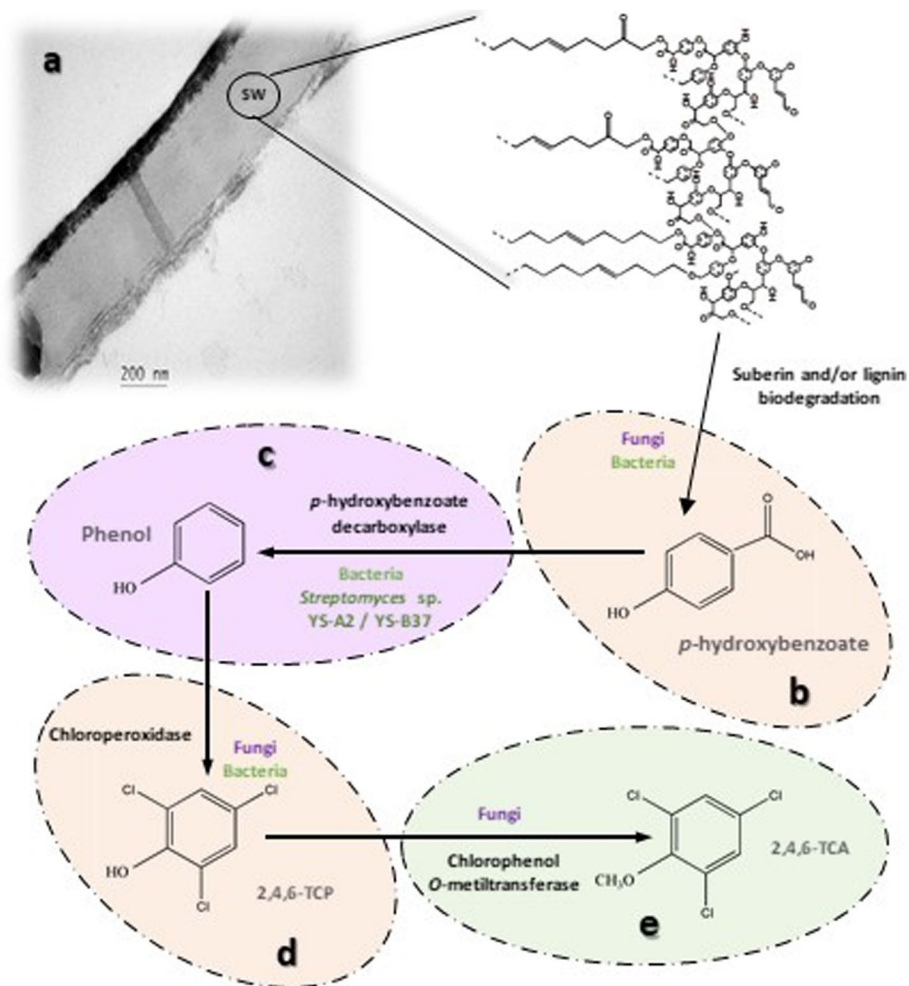


Fig. 9 Explanatory diagram of the processes involved in the formation of chlorophenols and chloroanisoles in cork. **a, b** Microbial degradation of suberin and/or lignin present in the suberized secondary wall (SW) results in the formation of *p*-hydroxybenzoate. **c** This compound can be transformed into phenol by some bacterial strains, such as the two *Streptomyces* sp. strains described in this study. **d** Once formed, phenol can be chlorinated by fungal (or bacterial) chloroperoxidases to produce different chlorophenols, including 2,4,6-TCP. **e** Finally, the toxic 2,4,6-TCP is efficiently detoxified into 2,4,6-TCA by fungal chlorophenol O-methyltransferases

filamentous fungi and bacteria that are highly abundant in natural environments (Supplementary Table 8), such as soils [92]. A significant proportion of the filamentous fungi isolated from cork (70.59%) exhibited CPO activity (Table 1).

Although the biological role of CPOs remains uncertain, Barnett and colleagues [103] demonstrated that CPO is efficiently secreted at the tips of growing hyphae of the fungus *Curvularia inaequalis*. It has been suggested that its putative role could involve the generation of highly oxidative radicals and compounds such as HOCl, Cl⁻, ¹O₂, and OH*, which are capable of disrupting and oxidizing a variety of structures, such as the protective lignocellulose of plant tissues. This activity facilitates the penetration of fungal hyphae through plant material, contributing to degradation, as observed in YS. Commercial CPO from *C. fumago* was able to chlorinate phenol and monochlorophenols such as 2-CP and 4-CP to produce several CPs, including 2,4,6-TCP, the direct precursor of 2,4,6-TCA (Fig. 9). The bioconversion of 2,4,6-TCP by *O*-methylation could be carried out by many of the fungi inhabiting cork (reviewed by Zhou et al., 2024) [104], resulting in the final production of 2,4,6-TCA, which contaminates cork.

However, given the high complexity of the microbial populations inhabiting cork, other combinations are possible. We cannot rule out the possibility that once produced, phenol could alternatively undergo *O*-methylation to generate anisole, although at least the chorophenol *O*-methyltransferase (CPOMT) from *Trichoderma longibrachiatum* was not able to *O*-methylate phenol [23]. However, it cannot be excluded that some CPOMTs from other microorganisms may be able to carry out this reaction. Once anisole is formed, it can be chlorinated to produce 2,4,6-TCA in a chemical (not biological) reaction in the presence of chlorinated reagents, a process that could explain the formation of 2,4,6-TCA in drinking water [104, 105]. Alternatively, we could hypothesize that 2,4,6-TCA could be formed by CPO-mediated halogenation of anisole, although the CPO of *C. fumago* seems to have a reduced appetite for anisole as a substrate, and we did not observe chlorination of 2-CA and 4-CA when they were used as substrates. The purification of CPOs from fungal strains isolated from cork, combined with a detailed analysis of their substrate spectrum, could provide further insights into this issue. It is important to consider that these CPOs may exhibit varying affinities for other phenolic compounds when acting as substrates in their enzymatic activity.

Finally, we cannot ignore the implications of these findings for the chlorine cycle in the biosphere. Soils and decaying plant litter contain significant amounts of chlorinated aromatic polymers, and it has been previously

reported that CPOs are involved in the formation of chlorolignin compounds [102]. Our work supports this finding and suggests that CPOs are involved in the formation of CPs such that the presence of these pesticides in the environment is not only a consequence of human activity, as previously thought. This could also explain the presence of contamination by CPs in unpolluted environmental samples. Indeed, CPO-mediated chlorination of organic materials, such as cork or decaying wood, could be an important chlorine sink in nature. A similar process could explain the unpleasant moldy odor often detected in wooden buildings (particularly those abundant in northern European countries), which is attributed to the formation of 2,4,6-TCA from 2,4,6-TCP, which is used as a wood preservative [35], although this compound has long been banned in Europe. Instead, it is possible that slow but constant microbial degradation of wood lignin could produce 2,4,6-TCP via the mechanism described in this work in wooden buildings.

Conclusions

Cork affected by YS exhibits extensive structural alterations, accompanied by a microbial colonization rate at least four times greater than that observed in SC. The fungal population within the cork is notably characterized by a high proportion of potential lignin-degrading isolates, with up to 82.35% of these isolates capable of growing in a medium where lignin is the sole carbon source. Many of these fungi exhibit laccase or peroxidase activities, which are likely responsible for the degradation of lignin or the aromatic fraction of suberin. Metataxonomic analyses have revealed a significant enrichment of potential lignin-degrading filamentous fungi in YS, including genera such as *Mortierella*, *Mucor*, *Penicillium*, and *Umbeopsis*. Additionally, bacteria from the orders *Enterobacterales* and *Burkholderia-Paraburkholderia-Caballeronia* are prevalent, with the latter group particularly noted for containing species capable of degrading lignin and various aromatic compounds. Cork contains numerous extractable compounds, including *p*-hydroxybenzoate, which is produced through the microbial degradation of lignin or the aromatic fraction of suberin. This compound serves as a precursor to phenol in a reaction catalyzed by a *p*-hydroxybenzoate decarboxylase. This bioconversion has been detected in two bacterial isolates of the *Streptomyces* genus. Once produced, phenol can be chlorinated by chloroperoxidases to yield various chlorophenols, including 2,4,6-TCP, the direct precursor for the biosynthesis of 2,4,6-TCA via *O*-methylation, a reaction common among many fungi-inhabiting cork.

This study demonstrates that *de novo* synthesis of chlorophenolic pesticides, including 2,4,6-TCP, is possible in the environment from compounds formed during the microbial

biodegradation of lignin and/or suberin. This finding also provides an explanation for the higher levels of 2,4,6-TCA detected in YS. These insights challenge the prevailing paradigm that environmental contamination by chlorophenolic compounds is solely due to anthropogenic causes.

Supplementary Information

The online version contains supplementary material available at <https://doi.org/10.1186/s40168-024-02003-8>.

Supplementary Material 1. Supplementary Fig 1. Estimated values of viable filamentous fungi and bacteria isolated from standard cork and yellow stain samples

Supplementary Material 2. Supplementary Fig 2. Boxplot of the phenolic compounds identified in yellow stain cork samples analyzed by UHPLC–MS/MS (ESI–)

Supplementary Material 3. Supplementary Fig 3. Chromatogram, MS/MS spectra, and tentative compound for the feature 6.23_137.0244

Supplementary Material 4. Supplementary Table 1. Relative abundances of fungal ASVs, expressed as the mean \pm standard deviation (%) in Standard Cork (SC) and Yellow Stain (YS) samples

Supplementary Material 5. Supplementary Table 2. Relative abundances of bacterial ASVs, expressed as the mean \pm standard deviation (%) in Standard Cork (SC) and Yellow Stain (SC) samples

Supplementary Material 6. Supplementary Table 3. Estimation of the global effects of cork type (SC, YS) on the Chao1, Shannon, Gini-Simpson and Pielou's evenness indices of the fungal ASVs

Supplementary Material 7. Supplementary Table 4. Estimation of the global effects of cork type (SC, YS) on the Chao1, Shannon, Gini-Simpson and Pielou's evenness indices of the bacterial ASVs

Supplementary Material 8. Supplementary Table 5. Fungal ASVs with significant differential abundances (p -value < 0.01) between cork affected by yellow stain (YS) and standard cork (SC).

Supplementary Material 9. Supplementary Table 6. Bacterial ASVs with significant differential abundances (p -value < 0.01) between cork affected by yellow stain (YS) and standard cork (SC).

Supplementary Material 10. Supplementary Table 7. Fungal isolates identified in this study and their corresponding ITS1–5.8S–ITS2 sequences

Supplementary Material 11. Supplementary Table 8. Numbers of heme-dependent and vanadate-dependent protein sequences of putative chloroperoxidases (heme and Va, respectively) identified in microorganisms and deposited in the UniProt database, categorized by taxonomic groups up to the order level

Supplementary Material 12. Supplementary Table 9. Phenolic and phenylpropanoid pathway-related compounds looked for in features detected by mass spectrometry

Supplementary Material 13. Supplementary Table 10. Features detected whose m/z matches with some phenolic and phenylpropanoid pathway-related compounds

Supplementary Material 14. Supplementary Table 11. Bacterial isolates identified in this study and their corresponding 16S rRNA contig sequences

Authors' contributions

MR-M, IO, VF, JR, and JJRC developed the original work concept. MR-M, RC, CC-P, IO, RO-S, and JR developed methodology and performed experimental work. MR-M, IO, VF, and JJRC wrote the original draft of manuscript. MR-M, IO, VF, JR, and JJRC reviewed and edited the manuscript. VF and JJRC got the funding. All authors were given the opportunity to review the results and comment on the manuscript. The authors read and approved the final manuscript.

Funding

This work was supported by the companies Francisco Oller S. A. (Cassà de la Selva, Girona, Spain) and J. Vigas (Palafrugell, Girona, Spain). Both companies participate and are financed through the tractor project for the wine sector GRAPERTE (Transformación innovadora del camino del vino hacia un sector más digitalizado y sostenible). Both companies participate in the primary project "Investigación sobre el corcho y los procesos de producción de los tapones de corcho con el fin de su optimización como herramienta enológica." The project GRAPERTE has been financed by the Ministerio de Industria y Turismo (Call "Actuaciones de fortalecimiento industrial del sector agroalimentario dentro del Proyecto Estratégico para la Recuperación y Transformación Económica Agroalimentario) within the framework of the Recovery, Transformation and Resilience Plan, financed by the European Union – NextGenerationEU." Marina Ruiz-Muñoz was supported by a postdoctoral contract financed by the Ministry of Science and Innovation (MCIN), the State Investigation Agency (AEI) (DOI/<https://doi.org/10.13039/501100011033>), and by the European Union "NextGenerationEU"/Recovery Plant, Transformation and Resilience (PRTR). Rebeca Otero-Suárez was supported by a research technician contract financed by the Ministry of Science and Innovation (MCIN), the State Investigation Agency (AEI) (DOI/<https://doi.org/10.13039/501100011033>), and the European Union "NextGenerationEU"/Recovery Plant, Transformation and Resilience (PRTR). Carla Calvo-Peña was supported by a predoctoral contract from the Junta de Castilla y León and the European Social Fund (EDU/601/2020).

Availability of data and materials

The raw metagenomic sequences are available in the NCBI Sequence Read Archive (<http://www.ncbi.nlm.nih.gov/sra>) under the BioProject accession number PRJNA1145933. Specifically, the 16S rRNA gene sequences are available under the accession numbers SRX25670071 to SRX25670080, while the ITS rRNA sequences are available under the accession numbers SRX25670081 to SRX25670090. All other data, including 16S rRNA and ITS sequences obtained from microorganisms isolated from cork samples, are available as Supplementary Materials.

Declarations

Ethics approval and consent to participate

Not applicable.

Consent for publication

Not applicable.

Competing interests

The authors declare no competing interests.

Author details

¹Instituto de Investigación de La Viña y El Vino, Escuela de Ingeniería Agraria, Universidad de León, Avenida de Portugal, 41, León 24009, Spain. ²Laboratorio de Análisis del Aroma y Enología, Facultad de Ciencias, Química Analítica, Instituto Agroalimentario de Aragón-IA2 (Universidad de Zaragoza-CITA), Zaragoza 50009, Spain. ³Francisco Oller S. A, Cassà de La Selva, Gerona 17244, Spain.

Received: 13 August 2024 Accepted: 10 December 2024

Published online: 11 January 2025

References

1. Veloso S, Bonifácio L, Diogo E, Ramos AP, Magro A, Fernandes JP, et al. Stand factors related to sensory defects of cork planks. *Revista de Ciências Agrárias*. 2015;38:230–7.
2. Brazinha C, Fonseca AP, Pereira H, Teodoro OMND, Crespo JG. Gas transport through cork: modelling gas permeation based on the morphology of a natural polymer material. *J Memb Sci*. 2013;428:52–62.
3. Pereira H. The rationale behind cork properties: a review of structure and chemistry. *BioResources*. 2015;10:1–23.
4. Pereira H. Cork chemical variability. *BioResources*. 2013;8:2246–56.

5. Chen Z, Wan C. Biological valorization strategies for converting lignin into fuels and chemicals. *Renew Sustain Energy Rev.* 2017;73:610–21.
6. Kamimura N, Sakamoto S, Mitsuda N, Masai E, Kajita S. Advances in microbial lignin degradation and its applications. *Curr Opin Biotechnol.* 2019;56:179–86.
7. Bugg TDH, Ahmad M, Hardiman EM, Rahmanpour R. Pathways for degradation of lignin in *Bacteria* and *Fungi*. *Nat Prod Rep.* 2011;28:1883.
8. Xu R, Zhang K, Liu P, Han H, Zhao S, Kakade A, et al. Lignin depolymerization and utilization by *Bacteria*. *Bioresour Technol.* 2018;269:557–66.
9. Woolfson KN, Esfandiari M, Bernards MA. Suberin biosynthesis, assembly, and regulation. *Plants.* 2022;11:555.
10. Graça J. Suberin: the biopolyester at the frontier of plants. *Front Chem.* 2015;3:62.
11. Borg-Olivier O, Monties B. Lignin, suberin, phenolic acids and tyramine in the suberized, wound-induced potato periderm. *Phytochem.* 1993;32:601–6.
12. Graça J. Hydroxycinnamates in suberin formation *Phytochem Rev.* 2010;9:85–91.
13. APCOR. Glossary - the vocabulary of cork. <https://www.apcor.pt/en/cork/facts-and-curiousities/glossary/>. 2023.
14. Rocha SM, Coimbra MA, Delgado I. Demonstration of pectic polysaccharides in cork cell wall from *Quercus suber* L. *J Agric Food Chem.* 2000;48:2003–7.
15. Rocha S, Delgado I, Ferrer Correia AJ, Poirier C. Etudes des attaques microbiologiques du liège *Quercus suber* L. *Rev Fr Oenol.* 1996;161:31–4.
16. Moio L, Diana M, Prete GD, Landa GD, Valentino AA, Bianco A. Analysis of volatiles of corks affected by yellow stain and greening and corked wines using GC-sniffing and GC/MS techniques. *Industrie delle Bevande.* 1998;27:615–9.
17. Álvarez-Rodríguez ML, López-Ocaña L, López-Coronado JM, Rodríguez E, Martínez MJ, Larriba G, et al. Cork taint of wines: role of the filamentous *Fungi* isolated from cork in the formation of 2,4,6-trichloroanisole by *O*-methylation of 2,4,6-trichlorophenol. *Appl Environ Microbiol.* 2002;68:5860–9.
18. Słabizki P, Legrum C, Wegmann-Herr P, Fischer C, Schmarr H-G. Quantification of cork off-flavour compounds in natural cork stoppers and wine by multidimensional gas chromatography-mass spectrometry. *Eur Food Res Technol.* 2016;242:977–86.
19. Tarasov A, Cabral M, Loisel C, Lopes P, Schuessler C, Jung R. State-of-the-art knowledge approximately 2,4,6-trichloroanisole (TCA) and strategies to avoid cork taint in wine. In: Morata A, Loira I, González C, editors. *Grapes and Wine*. IntechOpen; 2022. p. 337–66.
20. Taylor MK, Young TM, Butzke CE, Ebeler SE. Supercritical fluid extraction of 2,4,6-trichloroanisole from cork stoppers. *J Agric Food Chem.* 2000;48:2208–11.
21. Prak S, Gunata Z, Guiraud J-P, Schorr-Galindo S. Fungal strains isolated from cork stoppers and the formation of 2,4,6-trichloroanisole involved in the cork taint of wine. *Food Microbiol.* 2007;24:271–80.
22. Maggi L, Mazzoleni V, Fumi MD, Salinas MR. Transformation ability of *Fungi* isolated from cork and grape to produce 2,4,6-trichloroanisole from 2,4,6-trichlorophenol. *Food Addit Contam Part A.* 2008;25:265–9.
23. Coque J-JR, Álvarez-Rodríguez ML, Larriba G. Characterization of an inducible chlorophenol *O*-methyltransferase from *Trichoderma longibrachiatum* involved in the formation of chloroanisoles and determination of its role in cork taint of wines. *Appl Environ Microbiol.* 2003;69:5089–95.
24. Feltrer R, Álvarez-Rodríguez ML, Barreiro C, Godio RP, Coque J-JR. Characterization of a novel 2,4,6-trichlorophenol-inducible gene encoding chlorophenol *O*-methyltransferase from *Trichoderma longibrachiatum* responsible for the formation of chloroanisoles and detoxification of chlorophenols. *Fungal Genet Biol.* 2010;47:458–67.
25. Czaplicka M. Sources and transformations of chlorophenols in the natural environment. *Sci Total Environ.* 2004;322:21–39.
26. Garba ZN, Zhou W, Lawan I, Xiao W, Zhang M, Wang L, et al. An overview of chlorophenols as contaminants and their removal from wastewater by adsorption: a review. *J Environ Manage.* 2019;241:59–75.
27. Xia Q, Zhang XH. *Manual on water quality standards*. Beijing, China: China Environ Sci Press; 1990.
28. United States Environmental Protection Agency (USEPA). *Water Quality Criteria Summary, Ecological Risk Assessment Branch (WH-585) and Human Risk Assessment Branch (WH-550D)*. Washington, DC, USA: Health and Ecological Criteria Division; 1991.
29. Barakat AO, Kim M, Qian Y, Wade TL. Organochlorine pesticides and PCB residues in sediments of Alexandria Harbour. *Egypt Mar Pollut Bull.* 2002;44:1426–34.
30. Nyström A, Grimvall A, Krantz-Rüilcker C, Sävenhed R, Åkerstrand K. Drinking water off-flavour caused by 2,4,6-trichloroanisole. *Water Sci Technol.* 1992;25:241–9.
31. Jiang X, Martens D, Schramm K-W, Ketrup A, Xu SF, Wang LS. Polychlorinated organic compounds (PCOCs) in waters, suspended solids and sediments of the Yangtze River. *Chemosphere.* 2000;41:901–5.
32. Palm H, Knuutinen J, Haimi J, Salminen J, Huhta V. Methylation products of chlorophenols, catechols and hydroquinones in soil and earthworms of sawmill environments. *Chemosphere.* 1991;23:263–7.
33. D'Angelo EM, Reddy KR. Aerobic and anaerobic transformations of pentachlorophenol in wetland soils. *Soil Sci Soc Am J.* 2000;64:933–43.
34. McLellan I, Carvalho M, Silva Pereira C, Hursthouse A, Morrison C, Tatner P, et al. The environmental behaviour of polychlorinated phenols and its relevance to cork forest ecosystems: a review. *J Environ Monit.* 2007;9:1055.
35. Lorentzen JC, Juran SA, Ernstgård L, Olsson MJ, Johanson G. Chloroanisoles and chlorophenols explain mold odor but their impact on the Swedish population is attributed to dampness and mold. *Int J Environ Res Public Health.* 2020;17:930.
36. Lefebvre A, Riboulet JM, Boidron JN, Ribéreau-Gayon P. Incidence des microorganismes du liège sur les altérations olfactives du vin. *Sci Aliments.* 1983;3.
37. Jensen J. Chlorophenols in the terrestrial environment. In: Ware G, editor. *Reviews of environmental contamination and toxicology: Continuation of residue reviews*. New York: Springer; 1996. p. 25–51.
38. Maujean A, Millery P, Lemaesquier H. Explications biochimiques et metaboliques de la confusion entre gout de bouchon et gout de moisi. *Rev Fr Oenol.* 1985;25:55–62.
39. Álvarez-Rodríguez ML, Belloch C, Villa M, Uruburu F, Larriba G, Coque JJR. Degradation of vanillic acid and production of guaiacol by microorganisms isolated from cork samples. *FEMS Microbiol Lett.* 2003;220:49–55.
40. Serra R, Peterson S, Venâncio A. Multilocus sequence identification of *Penicillium* species in cork bark during plank preparation for the manufacture of stoppers. *Res Microbiol.* 2008;159:178–86.
41. Rodríguez-Andrade E, Stchigel AM, Guarro J, Cano-Lira JF. Fungal diversity of deteriorated sparkling wine and cork stoppers in Catalonia. *Spain Microorganisms.* 2019;8:12.
42. Veloso S, Magro A, Henriques J, Bonifácio L, Fernandes JP, Ramos AP, et al. *Trichoderma atroviride* associated with yellow stain defect of cork planks and critical values of TCA for wine cork stoppers industry. *Eur J Wood Prod.* 2024;82:1009–19.
43. Küster E, Williams ST. Selection of media for isolation of *Streptomyces*. *Nature.* 1964;202:928–9.
44. White TJ, Bruns T, Lee S, Taylor J. Amplification and direct sequencing of fungal ribosomal RNA genes for phylogenetics. In: Innis M, Gelfand D, Sninsky J, White T, editors. *PCR protocols: a guide to methods and applications*. New York: Academic Press, Inc.; 1990. p. 315–22.
45. Lane D. 16S/23S rRNA sequencing. In: Stackebrandt E, Goodfellow M, editors. *Nucleic acid techniques in bacterial systematics*. New York: John Wiley and Sons; 1991. p. 115–75.
46. Hall TA. BioEdit: a user-friendly biological sequence alignment editor and analysis program for Windows 95/98/NT. 1999. Available from: <https://api.semanticscholar.org/CorpusID:82421255>
47. Toju H, Tanabe AS, Yamamoto S, Sato H. High-coverage ITS primers for the DNA-based identification of *Ascomycetes* and *Basidiomycetes* in environmental samples. *PLoS ONE.* 2012;7: e40863.
48. Caporaso JG, Lauber CL, Walters WA, Berg-Lyons D, Lozupone CA, Turnbaugh PJ, et al. Global patterns of 16S rRNA diversity at a depth of millions of sequences per sample. *Proc Natl Acad Sci U S A.* 2011;108:4516–22.
49. Chen S, Zhou Y, Chen Y, Gu J. Fastp: an ultrafast all-in-one FASTQ pre-processor. *Bioinformatics.* 2018;34:i884–90.
50. Callahan BJ, McMurdie PJ, Rosen MJ, Han AW, Johnson AJA, Holmes SP. DADA2: high-resolution sample inference from Illumina amplicon data. *Nat Methods.* 2016;13:581–3.

51. Callahan BJ, McMurdie PJ, Holmes SP. Exact sequence variants should replace operational taxonomic units in marker-gene data analysis. *ISME J*. 2017;11:2639–43.
52. Martin M. Cutadapt removes adapter sequences from high-throughput sequencing reads. *EMBnet J*. 2011;17:10.
53. Nilsson RH, Larsson KH, Taylor AFS, Bengtsson-Palme J, Jeppesen TS, Schigel D, et al. The UNITE database for molecular identification of *Fungi*: handling dark taxa and parallel taxonomic classifications. *Nucleic Acids Res*. 2019;47:D259–64.
54. Quast C, Pruesse E, Yilmaz P, Gerken J, Schwier T, Yarza P, et al. The SILVA ribosomal RNA gene database project: improved data processing and web-based tools. *Nucleic Acids Res*. 2013;41:D590–6.
55. McMurdie PJ, Holmes S. PhyloSeq: an R package for reproducible interactive analysis and graphics of microbiome census data. *PLoS ONE*. 2013;8: e61217.
56. Pielou EC. The measurement of diversity in different types of biological collections. *J Theor Biol*. 1966;13:131–44.
57. Anderson MJ. A new method for non-parametric multivariate analysis of variance. *Austral Ecol*. 2001;26:32–46.
58. Oksanen J, Blanchet FG, Kindt R, Legendre P, Minchin PR, O'Hara RB, et al. *Vegan*: Community Ecology Package. 2012. Available from: <https://cran.r-project.org/package=vegan>.
59. Love MI, Huber W, Anders S. Moderated estimation of fold change and dispersion for RNA-seq data with DESeq2. *Genome Biol*. 2014;15:550.
60. Benjamini Y, Hochberg Y. Controlling the false discovery rate: a practical and powerful approach to multiple testing. *J R Stat Soc Series B Stat Methodol*. 1995;57:289–300.
61. R Core Team. R: a language and environment for statistical computing. R Foundation for Statistical Computing, Vienna, Austria [Internet]. 2023. Available from: <https://www.R-project.org>
62. Highley T. Changes in chemical components of hardwood and softwood by brown-rot *Fungi*. *Ser Agric Biol Environ Sci*. 1987;22:39–45.
63. More SS, Renuka PS, Pruthvi K, Swetha M, Malini S, Veena SM. Isolation, purification, and characterization of fungal laccase from *Pleurotus* sp. *Enzyme Res*. 2011;2011: 248735.
64. Shin KS, Kim CJ. Decolorization of artificial dyes by peroxidase from the white-rot fungus. *Pleurotus ostreatus* *Biotechnol Lett*. 1998;20:569–72.
65. Hadibarata T, Adnan LA, Yusoff ARM, Yuniarto A, Rubiyatno, Zubir MMFA, et al. Microbial decolorization of an azo dye reactive black 5 using white-rot fungus *Pleurotus eryngii* F032. *Water Air Soil Pollut*. 2013;224:1595.
66. Hunter-Cevera JC, Sotos L. Screening for a "new" enzyme in nature: haloperoxidase production by Death Valley dematiaceous *Hyphomycetes*. *Microb Ecol*: Springer-Verlag; 1986.
67. Shirling EB, Gottlieb D. Methods for characterization of *Streptomyces* species. *Int J Syst Bacteriol*. 1966;16:313–40.
68. Higgins CE, Hamill RL, Sands TH, Hoehn MM, Davis NE, Nagarajan R, et al. The occurrence of deacetoxycephalosporin C in *Fungi* and *Streptomyces*. *J Antibiot (Tokyo)*. 1974;27:298–300.
69. Wang K, Huang X, Lin K. Multiple catalytic roles of chloroperoxidase in the transformation of phenol: products and pathways. *Ecotoxicol Environ Saf*. 2019;179:96–103.
70. Crouvisier-Urien K, Chanut J, Lagorce A, Winckler P, Wang Z, Verboven P, et al. Four hundred years of cork imaging: new advances in the characterization of the cork structure. *Sci Rep*. 2019;9:19682.
71. O'Keefe J. Measuring biological diversity. *Afr J Aquat Sci*. 2004;29:285–6.
72. Ortiz-Burgos S. Shannon-Weaver Diversity Index. In: Kennish MJ, editor. *Encyclopedia of Estuaries*. Encyclopedia of Earth Sciences Series. Dordrecht: Springer; 2016. https://doi.org/10.1007/978-94-017-8801-4_233.
73. Caporaso JG, Lauber CL, Walters WA, Berg-Lyons D, Lozupone CA, Turnbaugh PJ, et al. Global patterns of 16S rRNA diversity at a depth of millions of sequences per sample. *PNAS*. 2011;108:4516–22.
74. Zhang W, Ren X, Lei Q, Wang L. Screening and comparison of lignin degradation microbial consortia from wooden antiques. *Molecules*. 2021;26:2862.
75. Ali NS, Huang F, Qin W, Yang TC. A high throughput screening process and quick isolation of novel lignin-degrading microbes from large number of animal biomasses. *Biotechnol Rep*. 2023;39: e00809.
76. Rodríguez A, Carnicero A, Perestelo F, de la Fuente G, Milstein O, Falcón MA. Effect of *Penicillium chrysogenum* on lignin transformation. *Appl Environ Microbiol*. 1994;60:2971–6.
77. Yang J, Yuan H, Wang H, Chen W. Purification and characterization of lignin peroxidases from *Penicillium decumbens* P6. *World J Microbiol Biotechnol*. 2005;21:435–40.
78. Zeng GM, Yu HY, Huang HL, Huang DL, Chen YN, Huang GH, et al. Laccase activities of a soil fungus *Penicillium simplicissimum* in relation to lignin degradation. *World J Microbiol Biotechnol*. 2006;22:317–24.
79. Ham Y, An J-E, Lee SM, Chung S-H, Kim SH, Park M-J. Isolation and identification of *Fungi* associated with decay of *Quercus mongolica*. *JKWST*. 2021;49:234–53.
80. Dobritsa AP, Samadpour M. Transfer of eleven species of the genus *Burkholderia* to the genus *Paraburkholderia* and proposal of *Caballeronia* gen. nov. to accommodate twelve species of the genera *Burkholderia* and *Paraburkholderia*. *Int J Syst Evol Microbiol*. 2016;66:2836–46.
81. Brink DP, Ravi K, Lidén G, Gorwa-Grauslund MF. Mapping the diversity of microbial lignin catabolism: experiences from the eLignin database. *Appl Microbiol Biotechnol*. 2019;103:3979–4002.
82. Tu Z, Geng A, Xiang Y, Zayas-Garriga A, Guo H, Zhu D, et al. Lignin degradation by *Klebsiella aerogenes* TL3 under anaerobic conditions. *Molecules*. 2024;29:2177.
83. Xu Z, Qin L, Cai M, Hua W, Jin M. Biodegradation of kraft lignin by newly isolated *Klebsiella pneumoniae*, *Pseudomonas putida*, and *Ochrobactrum tritici* strains. *ESPR*. 2018;25:14171–81.
84. DeAngelis KM, Sharma D, Varney R, Simmons B, Isern NG, Markillie LM, et al. Evidence supporting dissimilatory and assimilatory lignin degradation in *Enterobacter lignolyticus* SCF1. *Front Microbiol*. 2013;4:280.
85. Tian J-H, Pourcher A-M, Peu P. Isolation of bacterial strains able to metabolize lignin and lignin-related compounds. *Lett Appl Microbiol*. 2016;63:30–7.
86. Tao X, Feng J, Yang Y, Wang G, Tian R, Fan F, et al. Winter warming in Alaska accelerates lignin decomposition contributed by *Proteobacteria*. *Microbiome*. 2020;8:84.
87. Santos SAO, Pinto PCRO, Silvestre AJD, Neto CP. Chemical composition and antioxidant activity of phenolic extracts of cork from *Quercus suber* L. *Ind Crops Prod*. 2010;31:521–6.
88. Marques AV, Pereira H, Meier D, Faix O. Quantitative analysis of cork (*Quercus suber* L.) and milled cork lignin by FTIR spectroscopy, analytical pyrolysis, and total hydrolysis. *Holzforschung*. 1994;48:43–50.
89. Lupoi JS, Singh S, Parthasarathi R, Simmons BA, Henry RJ. Recent innovations in analytical methods for the qualitative and quantitative assessment of lignin. *Renew Sustain Energy Rev*. 2015;49:871–906.
90. Matsui T, Yoshida T, Hayashi T, Nagasawa T. Purification, characterization, and gene cloning of 4-hydroxybenzoate decarboxylase of *Enterobacter cloacae* P240. *Arch Microbiol*. 2006;186:21–9.
91. Lupa B, Lyon D, Shaw LN, Sieprawska-Lupa M, Wiegell J. Properties of the reversible nonoxidative vanillate/4-hydroxybenzoate decarboxylase from *Bacillus subtilis*. *Can J Microbiol*. 2008;54:75–81.
92. Wever R, Barnett P. Vanadium chloroperoxidases: the missing link in the formation of chlorinated compounds and chloroform in the terrestrial environment? *Chem Asian J*. 2017;12:1997–2007.
93. Pérez-Terrazas D, González-Adrados JR, Sánchez-González M. Qualitative and quantitative assessment of cork anomalies using near infrared spectroscopy (NIRS). *Food Packag Shelf Life*. 2020;24: 100490.
94. Bekris F, Vasileiadis S, Papadopoulou E, Samaras A, Testemassis S, Gkizi D, et al. Grapevine wood microbiome analysis identifies key fungal pathogens and potential interactions with the bacterial community implicated in grapevine trunk disease appearance. *Environ Microbiome*. 2021;16:23.
95. Jin R, Liao H, Liu X, Zheng M, Xiong X, Liu X, et al. Identification and characterization of a fungal strain with lignin and cellulose hydrolysis activities. *Afr J Microbiol Res*. 2012;6:6545–50.
96. Wilhelm RC, DeRito CM, Shapleigh JP, Madsen EL, Buckley DH. Phenolic acid-degrading *Paraburkholderia* prime decomposition in forest soil. *ISME Communications*. 2021;1:4.
97. Morya R, Salvachúa D, Thakur IS. *Burkholderia*: an untapped but promising bacterial genus for the conversion of aromatic compounds. *Trends Biotechnol*. 2020;38:963–75.
98. Rudnitskaya A, Delgadillo I, Rocha SM, Costa A-M, Legin A. Quality evaluation of cork from *Quercus suber* L. by the electronic tongue. *Anal Chim Acta*. 2006;563:315–8.

99. Wang S, Bilal M, Hu H, Wang W, Zhang X. 4-Hydroxybenzoic acid—a versatile platform intermediate for value-added compounds. *Appl Microbiol Biotechnol*. 2018;102:3561–71.
100. Tsagogiannis E, Asimakoula S, Drainas AP, Marinakos O, Boti VI, Kosma IS, et al. Elucidation of 4-hydroxybenzoic acid catabolic pathways in *Pseudarthrobacter phenanthrenivorans* Sphe3. *Int J Mol Sci*. 2024;25:843.
101. Hofrichter M, Ullrich R. Heme-thiolate haloperoxidases: versatile biocatalysts with biotechnological and environmental significance. *Appl Microbiol Biotechnol*. 2006;71:276–88.
102. Ortiz-Bermúdez P, Hirth KC, Srebotnik E, Hammel KE. Chlorination of lignin by ubiquitous *Fungi* has a likely role in global organochlorine production. *PNAS*. 2007;104:3895–900.
103. Barnett P, Kruitbosch DL, Hemrika W, Dekker HL, Wever R. The regulation of the vanadium chloroperoxidase from *Curvularia inaequalis*. *BBA-Gene Struct Expr*. 1997;1352:73–84.
104. Zhou H, Xie Y, Wu T, Wang X, Gao J, Tian B, et al. Cork taint of wines: the formation, analysis, and control of 2,4,6-trichloroanisole. *Food Innov Adv*. 2024;3:111–25.
105. Zhang K, Zhou X, Zhang T, Mao M, Li L, Liao W. Kinetics and mechanisms of formation of earthy and musty odor compounds: chloroanisoles during water chlorination. *Chemosphere*. 2016;163:366–72.
106. Sumner LW, Amberg A, Barrett D, Beale MH, Beger R, Daykin CA, et al. Proposed minimum reporting standards for chemical analysis. *Metabolomics*. 2007;3:211–21.

Publisher's Note

Springer Nature remains neutral with regard to jurisdictional claims in published maps and institutional affiliations.